HYDROGEN STORAGE USING MG-MIXED METAL HYDRIDES

BY

CANAN ACAR

Submitted in partial fulfillment of the
requirements for the degree of
Master of Science in Chemical Engineering
in the Graduate College of the
Illinois Institute of Technology

Approved _____
Advisor

Chicago, Illinois
May 2010

ACKNOWLEDGMENT

First of all, I would like to express my sincere thanks to my thesis supervisor Dr. Hamid Arastoopour for his support and patience throughout my study. I wish to express my warm thanks to Dr. Alan Zdunek who has given continuous encouragement, clear-sighted suggestions and for his help during my study. It was also a privilege for me to work with him during the course of this thesis.

My sincere gratitude is due to my thesis committee members who devoted their valuable time to read and comment on my thesis.

Very special thanks to Patrick L. McCarthy, Gizem Uzturk, Burcu Baykal, Ipek Akinci, Derya Civelekoglu and all my friends for their friendship and support which has given me strength even when I am far away from them.

I would like to thank to Dr. Philip Nash for letting me use his laboratory equipments during my experimental work, Dr. Nader Aderangi for his help during my experimental studies and Dr. Said Al-Hallaj for believing in me from the beginning. Cordial thanks for Donna Ivy and Peg Murphy for their assistance and help.

Finally, I wish to thank my family for all their endless support, patience and encouragement throughout my life. Besides these, I would also express my great debt of gratitude to my family believing in me. This thesis is dedicated to my mom, dad and sister.

TABLE OF CONTENTS

Page

ACKNOWLEDGEMENT iii

LIST OF TABLES vi

LIST OF FIGURES viii

ABSTRACT ix

CHAPTER

1. INTRODUCTION 1

1.1. The Energy Problem 1
1.2. What is Hydrogen? 2
1.3. Applications of Hydrogen Economy 3
1.4. Comparison of Hydrogen with Other Fuels 4

2. REVIEW OF HYDROGEN STORAGE PROCESSES 7

2.1. Introduction 7
2.2. Gas Phase Hydrogen Storage 8
2.3. Liquid Phase Hydrogen Storage 11
2.4. Hydrogen Storage Using Carbon Nanotubes 12
2.5. Hydrogen Storage Using Metal Hydrides 13
2.6. Magnesium and Magnesium Based Alloys 21
2.7. Material Processing 23
2.8. Alloying Magnesium with Different Metals 25

3. EXPERIMENTAL SETUP, PROCEDURE, AND MATERIAL PREPARATION 29

3.1. Experimental Setup 29
3.2. Sample Preparation Procedure 31
3.3. Particle Size Determination Procedure 31
3.4. Experimental Procedures 33

4. ANALYSIS OF THE EXPERIMENTAL DATA 39

4.1. Assumptions 39
4.2. Gas Leak 40
4.3. Number of Moles of Hydrogen Absorbed During Charging . 40

4.4. Number of Moles of Hydrogen Desorbed During Discharging 42

5. RESULTS AND DISCUSSION 43

5.1. Gas Leak Test Results 43
5.2. Effect of Temperature on the Absorption/Desorption Capacity and Rate 44

6. CONCLUSIONS 56

7. RECOMMENDATIONS 57

BIBLIOGRAPHY 57

LIST OF TABLES

Table		Page
1.1	Fundamental Differences Between Petroleum and Hydrogen	4
1.2	Comparison of Energy and Emissions of Combustible Fuels	5
2.1	U.S. Department of Energy Hydrogen Storage Goals	7
2.2	Expectations and Technical Issues	9
2.3	Properties of Compressed Gas Storage and Glass Microspheres	11
2.4	Status and Potentials of Different types of Metal Hydrides	21
4.1	High Pressure Zone Volume Calculation	40
4.2	Sample Chamber Zone Volume Calculation	41
5.1	Summary of the Experimental Results Compared to the Literature at 300°C	47
5.2	Summary of the Experimental Results Compared to the Literature at 200°C	50
5.3	Summary of the Experimental Results Compared to the Literature at 100°C	51
5.4	Summary of the Experimental Results Compared to the Literature at 20°C	53

LIST OF FIGURES

Figure		Page
1.1	The Oil Issue	1
2.1	Energy and Gravimetric Densities of Various Hydrogen Storage Systems	8
2.2	A Typical Compressed H_2 Composite Tank	9
2.3	Photo of Glass Microspheres for H_2 Storage	10
2.4	Schematic Representation of Hydrogen Storage in Metal Hydrides	15
2.5	Metal Hydride Pressure Behavior	16
2.6	Schematic Representation of Phase Transition in Metal Hydrides	18
2.7	Typical Pressure Composition Isotherm (PCI) Curves for an Ideal Metal-H_2 System	19
2.8	Mechanical Treatment Methods	23
2.9	Schematic Representation of Ball Milling	24
2.10	Bulk Metal versus Smaller Particles	24
2.11	Comparison Between Mass and Volume Capacities of Various RM_n-Type Compounds	26
2.12	Comparison of the Desorption Rates of MgH_2 with Different Metal Oxide Catalysts	27
3.1	Hydrogen Absorption/Desorption Experiment Apparatus	30
3.2	Schematic of Hydrogen Absorption/Desorption Experiment Apparatus	31
3.3	Schematic of Laser Diffraction Particle Sizing	33
5.1	Leak Test Result at 300°C	44
5.2	The Effect of Temperature on Hydrogen Storage Capacity of the Sorbent	45
5.3	The Effect of Temperature on Hydrogen Storage Rate of the Sorbent	46
5.4	Absorption and Desorption PCI Curves at 300°C	49
5.5	Absorption and Desorption PCI Curves at 200°C	50

5.6 Absorption and Desorption PCI Curves at 100°C 52
5.7 Absorption and Desorption PCI Curves at 20°C 54

ABSTRACT

Persistent urban air pollution, demand for zero or low emission vehicles and the need to reduce foreign oil imports have been enhanced the need for renewable energy alternatives. Hydrogen is a promising material since it is an environmentally harmless energy carrier. The lack of satisfactory hydrogen storage systems which are safe, cheap and simple is one of the main problems for the transition to a hydrogen-based energy system. Mg-based alloys show potential as hydrogen storage material because of the high gravimetric density of MgH_2 (7.6 wt. %), as well as its abundant supply and low cost as a raw material. However, they exhibit high enthalpies of formation, poor hydrogenation/dehydrogenation kinetics, poor charge/discharge cycling stability and high temperature requirements. Also, MgO formation and a high dissociation barrier of clean magnesium surfaces are other major problems with Mg-based alloys. These problems could be solved by mixing Mg with another chemical component, adding a small amount of a catalytically active metal on the surface of the Mg clusters and using smaller particle sizes [11]. The addition of $LaNi_5$ to MgH_2 reduced the temperature of hydrogen absorption, accelerated the kinetics at room temperature and yielded higher hydrogen storage capacity at elevated temperatures [3]. Furthermore, literature studies showed that Nb_2O_5 is the most effective catalyst for the hydrogen sorption reaction of Mg [4].

In this work, MgH_2-$LaNi_5$-Nb_2O_5 composite systems were prepared and studied to obtain a better understanding of hydrogen storage capacity and adsorption/desorption rates. Hydrogen storage capacities of our sorbent were measured by performing adsorption/desorption experiments at different temperatures.

The results of our experimental data were analyzed and compared with available data from the literature. The results of our experiments showed that alloying MgH_2 and $LaNi_5$-Nb_2O_5 increases the hydrogen absorption/desorption capacity and

rate at all temperature ranges. The advantages of our novel sorbent are observed more prominently at lower temperatures.

CHAPTER 1

INTRODUCTION

1.1 The Energy Problem

For many years, scientists have been discussing the environmental effects of fossil fuels and carbon based economy. For instance, in the UK 90 % of carbon dioxide and 83 % of other greenhouse gas emissions come from the production and use of energy, with 5.2 % of carbon dioxide and 7.1 % of greenhouse gas emissions agriculture and animal farming industries come next [34]. It is widely known that the release of CO_2 contributes to the global warming. According to UK Department of Business, Innovation and Skills, there has been a 1°C rise in global temperature in the last 150 years and there will be more increase if the world keeps using traditional carbon based energy sources [15]. Most of the countries in the world realized there will be more problems and chaos in the future and they signed the Kyoto protocol, to reduce emissions below 1990 levels. To meet these targets, a transition to a less polluting and carbon based source of energy is required.

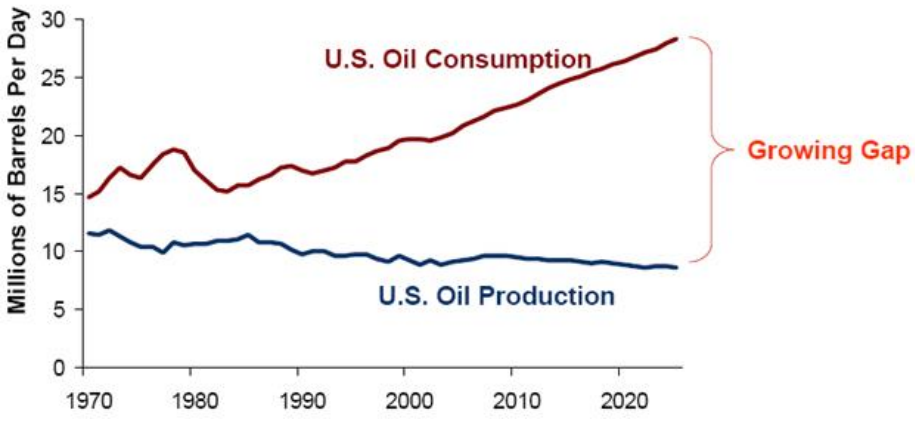

Figure 1.1. The Oil Issue

Finite nature, increasing demand and the political uncertainties of the fossil fuel sources result in a highly unstable price and financial concern over energy in the

future [40]. The growing gap between the oil consumption and production in the USA shown in Figure 1.1 indicates that the USA is becoming more dependent on foreign oil imports. Most of the fossil fuel production areas may be at their peak and their production levels are expected to decrease over the next twenty years [7][19]. It is predicted that fossil fuel will be available only in the most politically unstable regions in the coming years. And the oil may be depleted by 2040 and gas twenty years after that [15]. Because of all those financial problems, our dependence on oil-based products has to be stopped in the future.

Furthermore; persistent urban air pollution, demand for zero or low emission vehicles and the need to reduce foreign oil imports increase the need for renewable energy concept. In order to use those energy sources; safe, cheap, efficient and simple storage methods should be developed to solve the sporadic and sometimes unpredictable behavior of the renewable energy sources [35].

Hydrogen is a promising environmentally harmless energy carrier since it is carbon and sulfur-free. Therefore; an efficient, cheap and clean hydrogen production way has to be found. Furthermore; fueling infrastructure, consumer acceptance, and a strategy for its dependence on energy sources are needed as initial steps of hydrogen based economy [39].

1.2 What is Hydrogen?

Hydrogen, represented by the chemical symbol H, is the simplest, lightest chemical element known to man with atomic number 1. At standard temperature and pressure, hydrogen is a colorless, odorless, nonmetallic, tasteless, highly flammable diatomic gas with the molecular formula H_2.

Although hydrogen is the most abundant chemical element, constituting roughly 75 % of the universe's elemental mass, elemental hydrogen is relatively rare on Earth.

It is in the form of water when combined with oxygen (H_2O) and different compounds such as methane (CH_4), coal and petroleum when combined with carbon. It can also be found in biomass, and all living organisms.

Hydrogen cannot be mined or pumped from the ground; unlike oil, coal, or gas. It can only be obtained when an external energy source is used to extract it. Therefore, hydrogen can be described as an energy vector (like electricity). Using renewable energies to extract hydrogen from water allows renewable energies to be stored with zero carbon and greenhouse emissions which is a major advantage in developing a sustainable economy based on renewable energy sources [14] [36].

Currently, fossil fuels are commonly used to produce hydrogen. Hydrogen can be produced from water by electrolysis at a greater cost than production from fossil fuels [22]. In order to have a more environment friendly system, renewable and CO_2-neutral processes should be developed [1].

If the capacity for hydrogen storage is improved to reach the national targets, the contribution of energy from renewable energies such as wind and solar could be increased. Storage and distribution are two major problems need to be solved before switching to hydrogen economy [1].

1.3 Applications of Hydrogen Economy

The use of hydrogen as a fuel is not a new idea. Town gas was used until the 1950s, which comprised 50% hydrogen. Hydrogen has also been used in the chemical, metal and food industries for decades. Man has gone to the moon using primarily hydrogen as energy carrier. The interest in hydrogen vehicles goes back to the 1800s. In recent years, the importance of hydrogen has been realized by the major motor manufacturers, oil companies and importantly governments and those people from different industries are considering programs based on hydrogen energy [1].

The primary usage of hydrogen is currently limited to chemical, metal and food industries. But, hydrogen is becoming more popular everyday. For example, hydrogen gas turbines are also becoming more commercially viable. The versatility of hydrogen combined with little or no polluting emissions at end use makes it more important for a low carbon sustainable future. Hydrogen produced from sustainable renewable sources can provide a solution to the renewable energy storage problems and meet the growing needs of the transport sector [14]. Internal combustion (IC) engines are another area that use hydrogen.

Since the combustion of hydrogen to produce energy and its use in fuel cells to generate electricity produce only water, and a small amount of NO_x if it is burnt in air; it is currently being considered as the fuel of the future [32]. Hydrogen can be used both in transport and static applications to provide electricity and heat.

One of the main applications of the hydrogen is fuel cells. Fuel cells can be used in transportation instead of the IC engines. The fuel cell combines hydrogen and air and produces water, electricity and heat. Fuel cells have no moving parts and they are more quiet than traditional engines. They are three times as efficient as traditional combustion engines in peak operating conditions. Therefore, they can make hydrogen economically feasible [23].

1.4 Comparison of Hydrogen with Other Fuels

Table 1.1. Fundamental Differences Between Petroleum and Hydrogen

Petroleum	Hydrogen
Long, complex molecule	Extremely simple
Difficult to process	Easy to generate
Large refineries	Scalable, local
Combustion	Electrochemical
Easy to transport as liquid	Very hard to store/transport as liquid/gas

When comparing different fuels, their emissions at end use, life cycle evaluations from well to wheel, energy needed to retrieve them, relative energy inputs needed to create the final product and their transition through processing are taken into account. There are also other comparisons that can be made by looking at the emergy or exergy of the fuel; which give us an additional method of evaluating and making a realistic comparison between fuels. In Table 1.1, several advantages and disadvantages of hydrogen and petroleum are compared. From Table 1.1, it can be seen that although hydrogen has an extremely simple structure and it is easy to generate without the need of a complicated infrastructure, the storage and transportation problems need to be solved in order to move to a hydrogen-based economy.

Table 1.2. Comparison of Energy and Emissions of Combustible Fuels

Fuel Type	Energy per Mass (MJ/kg)	Energy per Volume (MJ/l) (approx.)	kg of Carbon Release per kg of Fuel Used
Hydrogen Gas	120	2	0
Hydrogen Liquid	120	8.5	0
Coal (anthracite)	15-19	-	0.5
Coal (sub-bituminous)	27-30	-	0.7
Natural Gas	33-50	9	0.46
Petrol	40-43	31.5	0.86
Oil	42-45	38	0.84
Diesel	42.8	35	0.9
Bio-diesel	37	33	0.5
Ethanol	21	23	0.5
Charcoal	30	-	0.5
Agricultural Residue	10-17	-	0.5
Wood	15	-	0.5

Table 1.2 compares the energy per unit mass, energy per unit volume and carbon dioxide emissions produced from combustion of different fuels (all the data

relate to the end use of the fuel). Table 1.2 shows that hydrogen is an effective energy carrier when compared with petrol or natural gas, the energy released per unit mass being twice that of traditional fuels [28].

Table 1.2 also shows that the energy per unit volume of both liquid and gas hydrogen is lower than all the other fossil fuels [28].

Also, by looking at Table 1.2, it can be concluded that hydrogen used in transportation has no carbon emissions [20] [9].

Vehicles need light, compact, safe and affordable system for on-board energy storage. A modern, commercially available car optimized for mobility and not prestige with a range of 400 km burns about 24 kg of petrol in a combustion engine; to cover the same range, 8 kg hydrogen are needed for the combustion engine version or 4 kg hydrogen for an electric car with a fuel cell.

CHAPTER 2

REVIEW OF HYDROGEN STORAGE PROCESSES

2.1 Introduction

Storage is one of the most challenging technical issues in moving towards the hydrogen economy. In order to use hydrogen as a future fuel, a cheap, safe and simple storage method should be developed. These storage methods need to have both high gravimetric density and volumetric density. Table 2.1 shows United States storage targets from the Department of Energy. The cost of transportation is related to the storage density.

Table 2.1. U.S. Department of Energy Hydrogen Storage Goals

Storage Parameter	Units	2005	2010	2015
Specific Energy	kWh/kg	1.5	2.0	3.0
	kg H_2/kg System	0.045	0.06	0.09
Energy Density	kWh/l	1.2	1.5	2.7
	g H_2/l	36	45	81
Storage System Cost	\$/kWh	6	4	2
	\$/kg H_2 Capacity	200	133	67
Refueling Rate	kg H_2/min	0.5	1.5	2.0
Cycle Life	Cycles (1/4 to full)	500	1000	1500

Compressed gas, liquid form and metal hydrides are the main options for storing hydrogen. The gravimetric and volumetric densities of different hydrogen storage options at various temperatures and pressures are shown in Figure 2.1. However, there is no commercially produced storage has achieved the targets in Table 2.1 yet. Each alternative has advantages and disadvantages. For example, liquid hydrogen has a high storage density, but it also requires an insulated storage container and energy intensive liquefaction process.

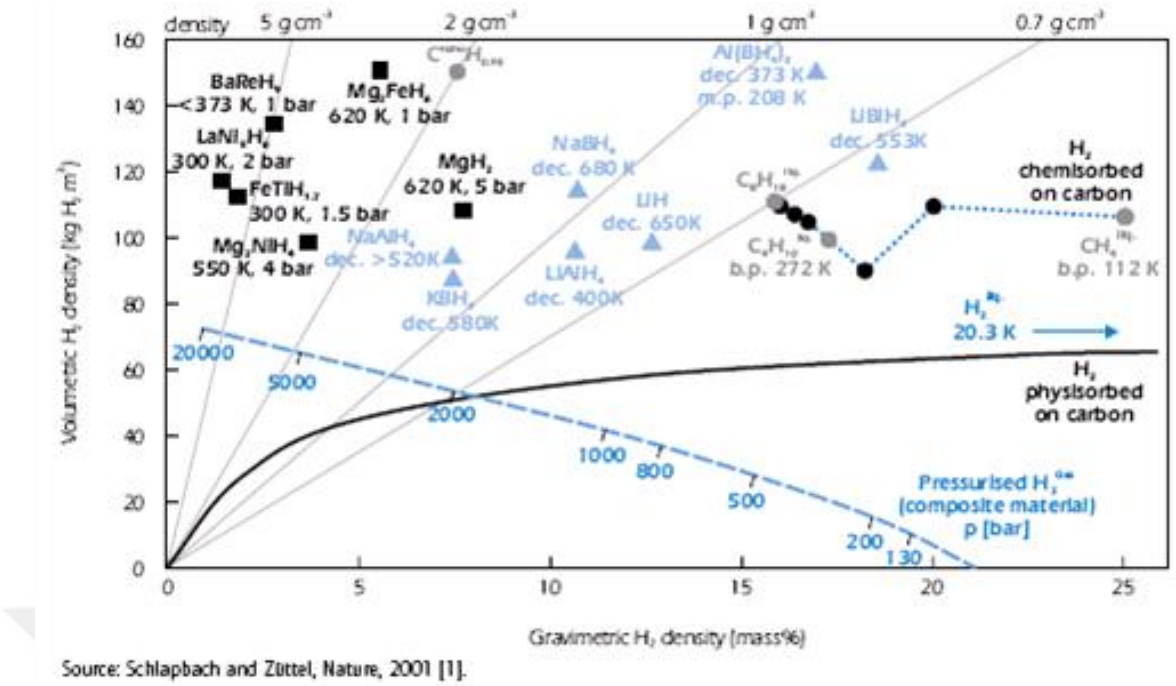

Figure 2.1. Energy and Gravimetric Densities of Various Hydrogen Storage Systems

Another challenging goal is to be able to recharge the system in 3 minutes (one of the targets in Table 2.1). For example, a typical 5 kg H_2-hydride bed, would require 500 kW of heat removal during charging which might cause the need of an off board charging [24].

It should be noted that all H_2 storage systems, except gaseous systems, require a heat exchanger. Heat must be generally removed during recharging and added during discharging. Waste heat from the fuel cell or internal combustion engine (ICE) should be utilized in order to make the system more efficient [24].

Table 2.2 shows the expectations from future hydrogen storage systems and the technical issues to be solved to reach the targets in Table 2.1.

2.2 Gas Phase Hydrogen Storage

Steel tanks, lightweight composite tanks, cryogas, and glass microspheres are

Table 2.2. Expectations and Technical Issues

Expectations	Technical Issues
Safety	Weight
Low weight	Volume
Low cost	Discharge rate
Abundance	Heat requirements
Low enthalpy of formation	Recharging time
Good reversibility	Cost
High capacity	
Fast reactivity	

the main options to store hydrogen in gaseous form. Currently, steel tank is the most common method but lightweight composite tanks are also becoming popular since they are designed to stand at higher pressures. Cryogas, hydrogen cooled near cryogenic temperatures, can be used to increase the volumetric energy density. Using glass microspheres is a novel method to store hydrogen at high pressures [24]. Hydrogen diffuses through the thin walls of the glass microspheres at elevated temperatures and pressures. The gas is then trapped upon cooling to room temperature.

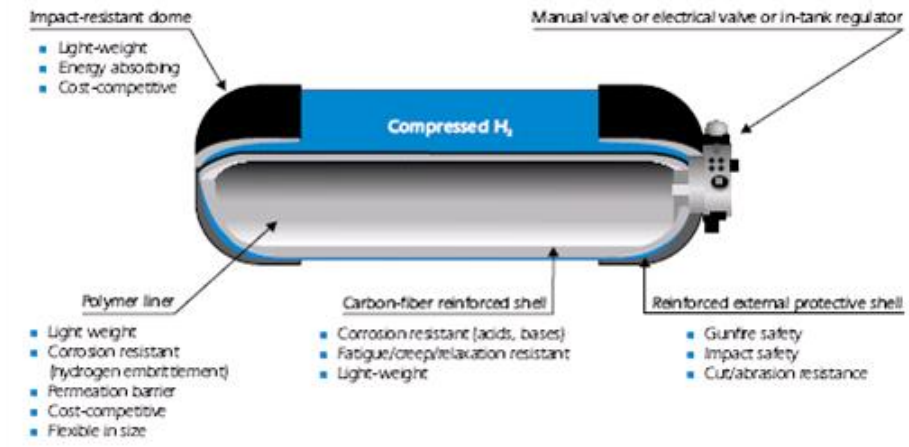

Figure 2.2. A Typical Compressed H_2 Composite Tank

Because the only equipment required is a compressor and a pressure vessel,

compressed gas storage of hydrogen is the simplest storage solution. Other advantages of compressed gas storage in composite tanks include: low weight which meets the DOE targets, commercial availability, well-engineered and safety-tested tanks available with existing extensive prototyping experience and no need for an internal heat exchange. Compressed gas storage also meets codes that are accepted in several countries for pressures in the range of 350-700 bar. However; they require larger physical volumes than DOE targets, the ideal cylindrical shape makes it difficult to conform to available spaces, they have a high cost (500-600 USD/kg H_2), and there are energy penalties associated with compressing the gas to very high pressures which can be stated as the main disadvantages. Also, rapid loss of H_2 in an accident can be a big safety problem [24]. The most important problem is the low volumetric density which depends on the storage pressure. Higher pressures can increase the storage capacity, but it will also result higher capital and operating costs and safety issues [17]. The long-term effect of hydrogen on the materials under cyclic or cold conditions is also not fully understood.

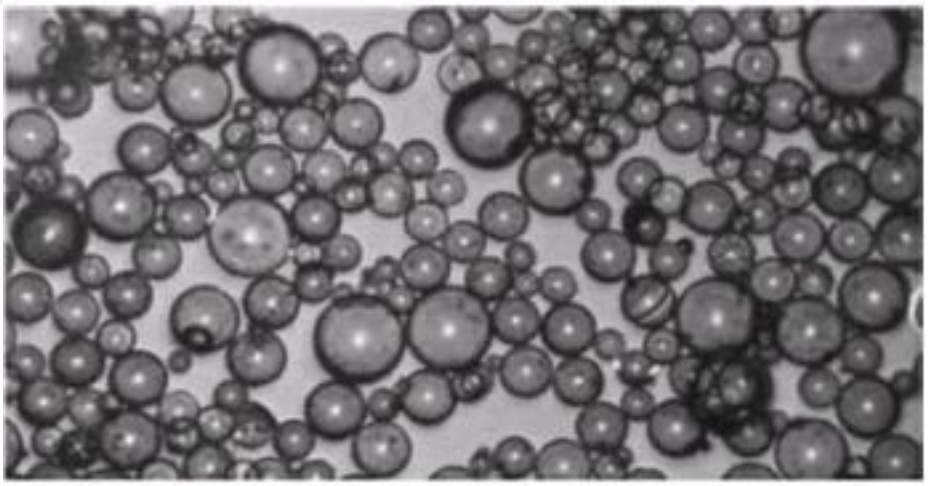

Figure 2.3. Photo of Glass Microspheres for H_2 Storage

Glass microspheres method has low container costs since it has the potential to be inherently safe as they store H_2 at a relatively low pressure onboard and are

suitable for conformable tanks (see Figure 2.3). The significant technical advantage is the demonstrated storage density of 5.4 wt. % of H_2 [24]. However, glass microspheres have low volumetric density and high pressures is needed for filling and there is a slow leak of hydrogen at ambient temperatures. Another problem is the breakage of glass microspheres during cycling. The main problem is the need to supply heat at temperatures higher than the temperature which is available from the PEM fuel cell (ca. 70-80°C). The high temperature required (ca. 300°C) also makes rapid response-control difficult.

Table 2.3 compares the temperature and pressure requirements of composite tank and glass microspheres hydrogen storage options. Also, the comparison of robustness, safety, cost and energy density of those two gas phase hydrogen storage options are mentioned in Table 2.3.

Table 2.3. Properties of Compressed Gas Storage and Glass Microspheres

	Composite Tanks		Glass Microspheres	
Parameter	Value	Comment	Value	Comment
Temperature (T)	+	No heat exchanger	-	High T needed
Pressure (P)	-	High P compressors needed	+	Low onboard P possible
Energy Density	-	Only partially conformable	+	Up to 5 wt. % H_2, conformable
Robustness	+	Extensively tested	-	Breakable spheres
Safety	+	Existing codes & standards	+	Inherently safe
Cost	-	500-600 USD/kg H_2	?	Needs to be determined

2.3 Liquid Phase Hydrogen Storage

Liquefaction is a process done by using a combination of compressors, heat exchangers, expansion engines, and throttle valves to cool a gas to form a liquid [16].

The most important problem about liquid hydrogen is the need of insulation

and heat transfer which results in evaporation of hydrogen and boiling of the liquid. Because of the work required to liquefy hydrogen, any evaporation causes a net loss in system efficiency but there will be an even greater loss if the hydrogen is released to the atmosphere instead of being recovered.

Well-insulated cryogenic containers, spherical tanks (to decrease the surface area for heat transfer per unit volume), and larger tanks (as the diameter increases volume increases faster than the surface area) can be used to minimize boil-off [16] [18]. Cylindrical tanks might also be used instead of spherical ones since they are cheaper to produce than spherical tanks and have almost similar volume - to surface area ratio [16].

2.4 Hydrogen Storage Using Carbon Nanotubes

Carbon nanotubes are allotropes of carbon with a cylindrical nanostructure. Nanotubes have significantly high length-to-diameter ratio and these cylindrical carbon molecules have novel properties that make them potentially useful in many applications.

Carbon nanotubes have shown promise for applications in hydrogen storage due to the electronic nature resulting from sp^2 hybridization, large surface areas, and molecular sized pores. Early experimental data for hydrogen storage in carbon nanomaterials was initially promising, indicating high hydrogen storage capacities exceeding DOE targets. However, the more recent experimental data obtained with different methods and on various carbon nanostructures are contradictory with large variance in the amount of hydrogen stored. And the general consensus today is that the high H_2-storage capacities (30-60 wt. %) reported a few years ago are impossible to reach and were the result of measurement errors [8].

Room temperature adsorption up to a few wt.% H_2 is occasionally reported,

but has not been reproducible. This requires a new bonding mechanism with energies between physisorption and strong covalent chemisorption. The surface and bulk properties needed to achieve practical room temperature storage are not clearly understood, and it is far from certain that useful carbon can be economically and consistently synthesized [8].

2.5 Hydrogen Storage Using Metal Hydrides

Although the actual meaning of hydride is a negative ion of hydrogen and it does not exist in ordinary conditions, the term hydride is used to describe compounds of hydrogen with other elements, particularly those of groups 1-16.

Since hydrogen is a highly reactive element, it forms one or more hydrides with every element of the periodic table except few noble gases. According to the nature of the bonding, these hydrides are divided into three main categories:

- Saline hydrides: they have significant ionic character
- Covalent hydrides: including the hydrocarbons and many other compounds
- Interstitial hydrides: they may be described as having metallic bonding

Metals behave like hydrogen sponge since they can absorb hydrogen in atomic form. About 50 metallic elements of the periodic table can absorb hydrogen in considerable quantities. By chemical bonding of hydrogen to metal or metalloid elements and alloys, metal hydrides are formed [30]. In metal hydrides, metal atoms behave like a host lattice and hydrogen atoms are trapped in the interstitial sites, such as lattice defects or vacancies [10] [43].

Metal hydrides offer an alternative to gas phase and liquid phase hydrogen storage systems. They allow hydrogen to be stored in solid form [13]. They are unique

because some of them can store hydrogen under moderate pressures. Depending on the alloy chosen, there is a wide operating range of pressures and temperatures [29]. Each alloy has different performance features like heat of reaction and cycle life. Possible choices of hydrogen storage using metals are enormous [11].

According to their reactivity towards hydrogen, pure metals may be classified as:

- Alkali metals, alkaline earths, early transition metals (e.g. zirconium (Zr), titanium (Ti), and magnesium (Mg)) or the rare earth metals (R-type elements) which form highly stable hydrides at room temperature.
- Late transition metals (e.g. chromium (Cr), iron (Fe), nickel (Ni)) or some p-elements (M-type elements) which do not form stable hydrides at room temperature.

Its H_2 equilibrium pressure at a given temperature determines the stability of the formed hydride [26].

Metal hydrides can be classified into two categories according to the temperature of absorption/desorption process:

- High temperature hydrides: higher storage capacities, low molecular weight materials with ionic bonding
- Low temperature hydrides: high molecular weight materials with covalent bonding

Since conventional hydrides require high temperatures to release hydrogen, their application to vehicles is not practical. There are some hydrides which release

hydrogen at low temperatures but they have lower gravimetric densities (3-5 wt. %) and higher weights than the conventional hydrides. They provide a good storage method where weight is not a problem [13].

Two possible ways of forming a metal hydride:

- direct dissociative chemisorptions

$$M + \frac{x}{2}H_2 \leftrightarrow MH_x \tag{2.1}$$

- electrochemical splitting of water: there has to be catalyst (i.e. palladium) to break down the water

$$M + \frac{x}{2}H_2O + \frac{x}{2}e^- \leftrightarrow MH_x + \frac{x}{2}OH^- \tag{2.2}$$

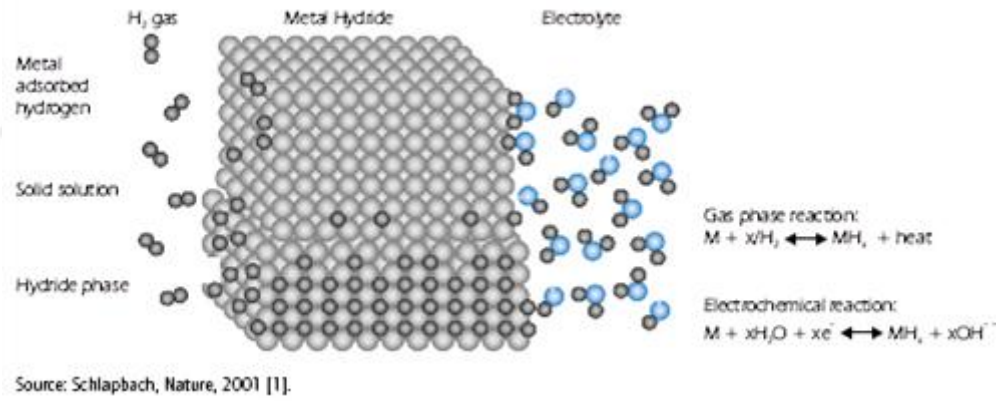

Figure 2.4. Schematic Representation of Hydrogen Storage in Metal Hydrides

The reactions are reversible and take place at moderate temperatures and pressures. Figure 2.4 shows the schematic representation of hydrogen storage in metal hydrides.

Fulfillment of thermodynamic and kinetic requirements is the necessary condition for hydrogen storage. The reactions usually have multiple steps, therefore failure

of one step may prevent the metal hydride reaching its thermodynamical equilibrium of hydrogen storage within a reasonable time. Because of this reason, the reaction rate of a metal-hydrogen system is a function of pressure and temperature [11].

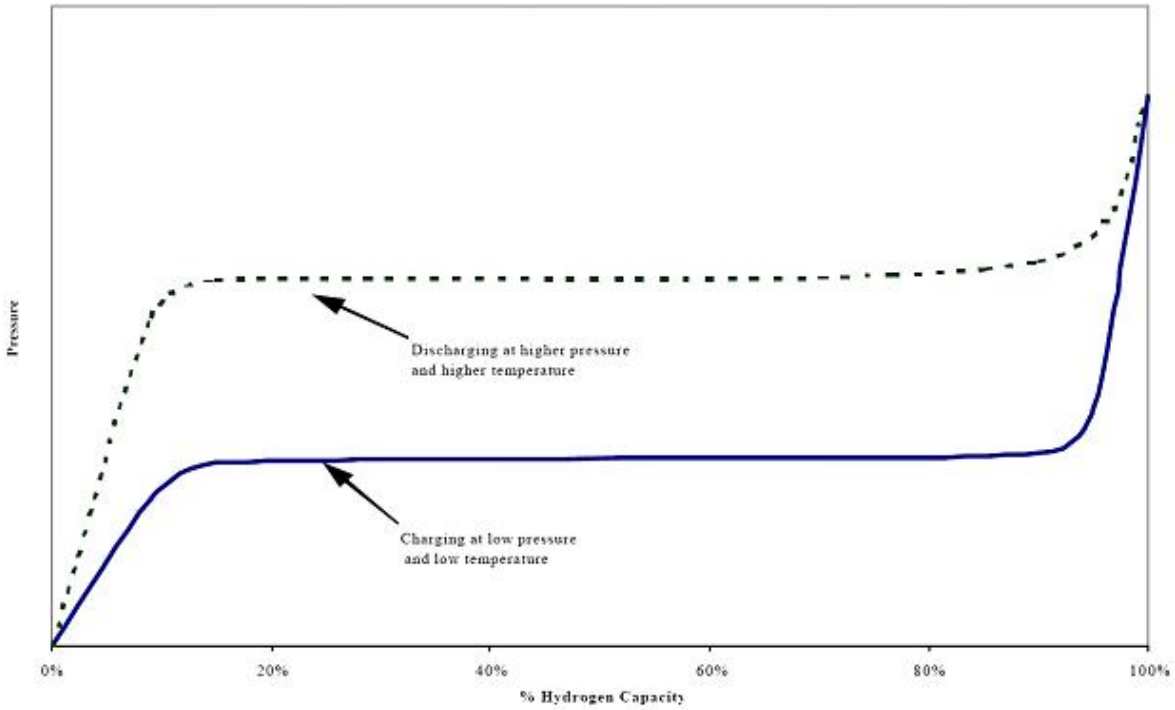

Figure 2.5. Metal Hydride Pressure Behavior

Pressure behavior of a typical metal hydride is shown in Figure 2.5. The hydrogen partial pressure first increases causing the hydrogen to dissolve in the metal or alloy, then hydrogen begins to bond to the metal. The equilibrium (or plateau) pressure stays constant during the bonding period (the time that 10 % of the hydrogen has been stored until about 90 % of the storage capacity is reached). Higher pressures are needed to reach 100 % after the 90 % point [41]. It is necessary to remove the heat released during hydride formation to prevent the hydride from heating up. Increasing temperature causes an increase in the equilibrium pressure until no more bonding occurs.

There are several activation barriers to overcome during chemical bonding of hydrogen to a solid structure (such as metal hydride). Near the surface it can absorb in a weak van de Waals interaction with the surface electrons through a small polarization of its electronic charge physisorption. If the kinetic energy is large enough for the H-H bond to stretch slightly (one activation barrier), its molecular bond can shift partly towards the surface and become more tightly bound to the surface (chemisorption). If the kinetic energy is so high that the H-H bond can be split (another activation barrier) and turned completely towards the surface, the hydrogen atoms can be dissociated and atomic chemisorbed to the surface, but only if there are two free sites at the surface [11].

Because of electronic and geometrical considerations, the filling of all available interstices in the metal lattice is never observed. Charge transfer between the hydrogen atom and the transition metal creates electric charge on the hydrogen atom that causes repulsive interaction which causes a minimum internuclear distance of about 2.1 A° between neighboring atoms. Also, if one considers the radius of the sphere tangent to the closest metallic atoms of the site assuming the atoms are hard spheres, the minimum radius of such an interstitial site must be larger than 0.40 A° to be filled by one hydrogen atom [26].

Hydrogenation reaction can be described as:

1. Incubation period: constant pressure period without any hydrogen absorption because of the passivation effect related to existence of metal oxide layers at the grain surface

2. Absorption: during this period, pressure variations observed indicating the reaction rate

3. Equilibrium: constant pressure period for a given temperature

There are two phases in hydride formation. In α-phase, only some hydrogen is adsorbed and in β-phase, hydride is fully formed. During charging period, hydrogen diffuses from the surface of the particle trough the β-phase interface and forms additional β-phase hydride. When discharging, hydrogen from the phase-transition interface diffuses through the α-phase to the surface of the particle where it is recombined into the form of molecular hydrogen [11]. Figure 2.6 shows the transition between α and β phases schematically.

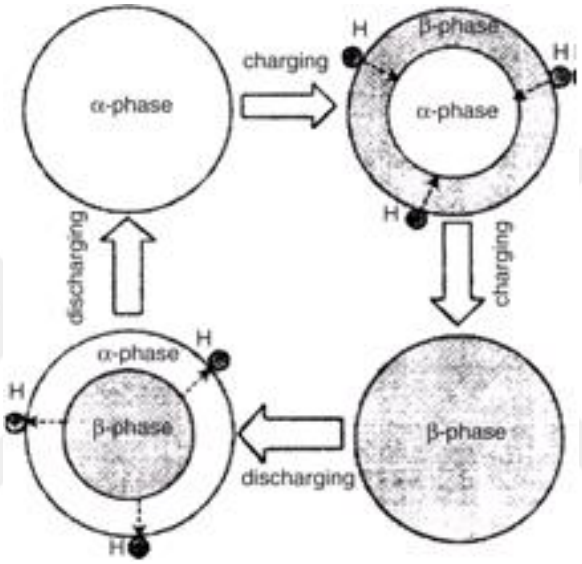

Figure 2.6. Schematic Representation of Phase Transition in Metal Hydrides

The transformation of the α-phase into the β-phase causes a plateau pressure below T_c. α-phase, a solid solution single phase domain, occurs at low H contents (x $< \alpha_{max}$ in H/M), and the hydrogen absorption/desorption can be shown as:

$$MH_x + \frac{dx}{2} H_2 \leftrightarrow MH_{x+dx} \tag{2.3}$$

Two phase domain occurs when $\alpha_{max} <$ x $< \beta_{min}$. When α-phase is saturated, x $= \alpha_{max}$, transformation into the β-phase starts with composition x $= \beta_{min}$ which causes the plateau pressure stay constant with increasing composition while the following

equilibrium reaction takes place

$$MH_x(\alpha_{max}) + \frac{y-x}{2} H_2 \leftrightarrow MH_y(\beta_{min}) \tag{2.4}$$

Since there is an extra energy needed to overcome the absorption barriers, the hydrogen equilibrium pressure is higher during absorption than desorption [26].

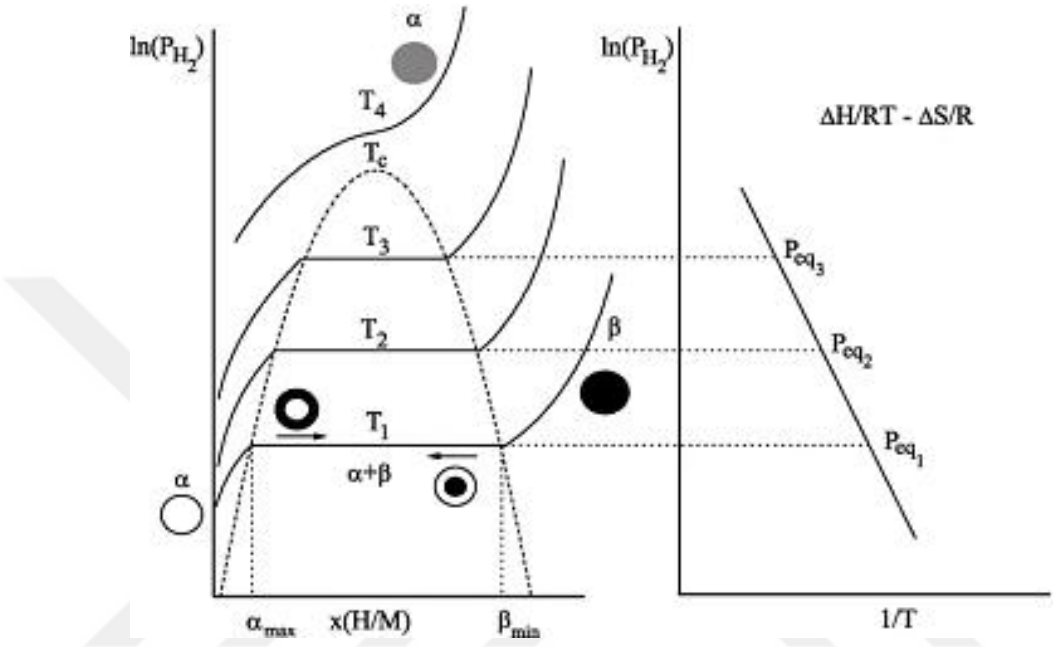

Figure 2.7. Typical Pressure Composition Isotherm (PCI) Curves for an Ideal Metal-H_2 System

PCI diagrams are used to illustrate the formation of a hydride by showing the formation of α-phase at low pressures and concentrations, growth of α phase and phase transformation from α to β phase at a certain constant plateau pressure with increasing concentration as shown in Figure 2.7 [11].

Heat must be added to break the bonds between the hydrogen and metal to release hydrogen. Higher release pressures are needed at higher temperatures. After a certain point, releasing hydrogen becomes more difficult and the last hydrogen molecules dissolved in the metal matrix are most difficult ones to remove because they have strong bounds that cannot be released during the normal charge/discharge

cycle [2]. According to some work, nickel plays a catalytic role for the hydrogen molecule dissociation [26]. The following equation shows how hydrogen is released from the metal hydride:

$$M + xH_2 \rightarrow MH_{2x} \tag{2.5}$$

Where M is the storage metal alloy and x is dependent on adsorptivity.

Metal oxides, hydroxides, carbon-oxygen compounds and water may cause a surface passivation layer during hydride formation. Since this passivation layer acts like a diffusion barrier and decreases the numbers of dissociation sites for H_2, it reduces the hydrogen uptake rate. Oxidation is the main reason causing a storage capacity decrease during a hydrogen absorption/desorption cycle. Alloy composition plays an important role in cycle life. Lanthanum replacement by mischmetal ($LaNi_5$) causes a substantial increase of the cycle life [26].Sometimes gaseous impurities in the reacting atmosphere can inhibit the hydrogen dissociation rate, which is also known as poisoning effect. Very strong (SO_2, H_2S and CH_3SH) and strong gaseous poisons (O_2, CO_2 and CO) has to be avoided, but CH_4, C_2H_4 and N_2 that have no measurable effect on the hydrogen absorption kinetics [11].

Although hydrogen storage in metal hydrides is a complex process with multiple steps depending on several parameters; many metals and alloys can store good amounts of hydrogen when safety, global yield and long term storage advantages are considered. But they must have light weight, high capacity, good reversibility, fast reactivity and sustainability to meet the hydrogen storage goals. Metal surfaces have to be able to release hydrogen and allow the hydrogen atoms to move easily. Another important expectation is they should dissociate the hydrogen molecules in a temperature range between 50 and 100°C. Therefore, surface structure, morphology and purity are other important factors affecting a metal's hydrogen absorption/desorption kinetics [11]. Corrosion, passivation, decrepitation, poor kinetics, and short cycle life

are the most common problems about metal hydrides.

Hydride systems based on existing metal hydrides cannot store large amounts of hydrogen and the development of new kinds of hydride materials is required.

Table 2.4. Status and Potentials of Different types of Metal Hydrides

Hydride Type	Status and Potential
Elements	Well characterized but unfavorable thermodynamics - too stable or too unstable to use at temperatures of 0-100°C.
Alloys & Intermetallic Compounds	Very well studied: many work well at temperatures less than 100°C, but with low gravimetric capacities for vehicles ($<$ 2.5 wt % H_2). Technically suitable for stationary storage, but rather expensive.
Nanocrystalline Amorphous	Good kinetics, unfavorable H_2 capacities and desorption temperatures.
Complex	Main hope for the future.

Table 2.4 summarizes the current status and potentials of different types of metal hydrides. Metal hydride complexes are the most promising hydrogen storage options compared to other metal hydride types.

2.6 Magnesium and Magnesium Based Alloys

Although the number of metal hydride choices are enormous, hydrogen storage system targets put some constraints on the chemical elements which can be used. Magnesium is a promising material since it forms a hydride(MgH_2) which provides up to 7.6 wt. % of hydrogen storage and this capacity is higher than all other known reversible metal hydrides. Their low cost, light weight and abundant supply are other advantages of magnesium hydrides. The high enthalpy of formation (ΔH= - 75 kJ/mole) of magnesium hydrides is advantageous for thermal energy storage.

The problems about magnesium hydrides can be stated as:

i. Slow hydrogenation/dehydrogenation: because of slow diffusion of hydrogen

atoms through the hydride

ii. Dissociation barrier: because hydrogen atoms do not readily dissociate at the surface of Mg, a catalyzer is needed for bond breaking and formation; transition metals are the best match, but main group elements do not work

iii. High enthalpy of formation: because hydrogen atoms bind too strongly to the Mg atoms, the hydride needs to be heated to very high temperature, around 350°C, in order to release hydrogen gas at high enough pressure (over 1 atm).

Although they both indicate the challenges about kinetics of absorption and desorption processes, (i) and (ii) are two different problems.

Using smaller Mg particles or mixing Mg with other chemical components like Ni could increase the hydrogenation/dehydrogenation rates and solve the first problem. Although the weight of Ni dramatically reduces the wt. % of hydrogen in the hydride, previous researches show that formation of nano-sized particles increases the hydriding/dehydriding kinetics [5].

Adding a small amount of catalytically active metal on the surface of Mg particles helps solving the dissociation (second) problem.

Since high enthalpy of formation causes high temperature requirements for desorption, third problem is the most serious one. Adding Ni to Mg decreases the desorption temperature but this is still far from being low enough. Also, adding heavy transition metals greatly reduces the hydrogen storage capacity of magnesium hydrides. Adding a light metal with low affinity to hydrogen would be a better solution to the third problem.

It is known that mechanically alloying Mg with other transition metals and producing fine particles in the submicrometer or even nanometer sizes can increase

the maximum solubility of hydrogen [5]. Also, both particle size and sample preparation methods affect the kinetics of the hydrogen absorption/desorption properties [33]. Therefore, the main goal of this research is to find an efficient way to improve absorption/desorption rates of magnesium hydrides and decrease the high temperature requirements by chemical alloying of magnesium with other components (Nb_2O_5 and $LaNi_5$) and material processing (ball-milling).

2.7 Material Processing

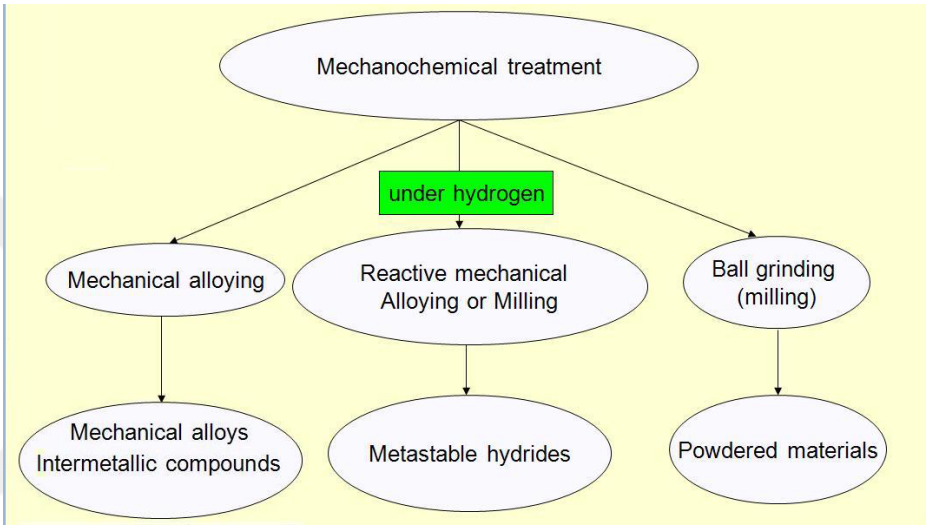

Figure 2.8. Mechanical Treatment Methods

As can be seen from Figure 2.8; mechanical alloying, reactive mechanical alloying or milling, and ball grinding (milling) are the main mechanical treatment methods.

Mechanical alloying can be used to produce extremely fine microstructure composite metal powders. Mechanical alloying helps two metals form a solid solution without the need for a high-temperature excursion. By the mechanical alloying method, an extremely fine dispersion of one of the metals in the other can be obtained even if the two metals are insoluble in the liquid or solid state.

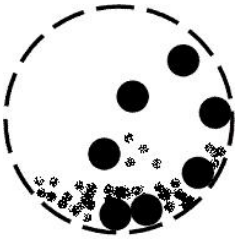

Figure 2.9. Schematic Representation of Ball Milling

Ball milling is a method of grinding and mixing different materials in a rotating cylinder or conical mill partially filled with grinding media such as balls or pebbles (see Figure 2.9). This process might or might not be in the presence of a liquid. The medium in the containers (argon, toluene, or tetrahydrofuran) affects the surface properties in a ball milling process [33].

As can be seen from Figure 2.10, bulk metal has long diffusion distances for hydrogen to penetrate which causes slow hydrogen exchange rates. But when this metal is processed into smaller particles, the diffusion distance for hydrogen gets shorter and it increases the hydrogen exchange rate.

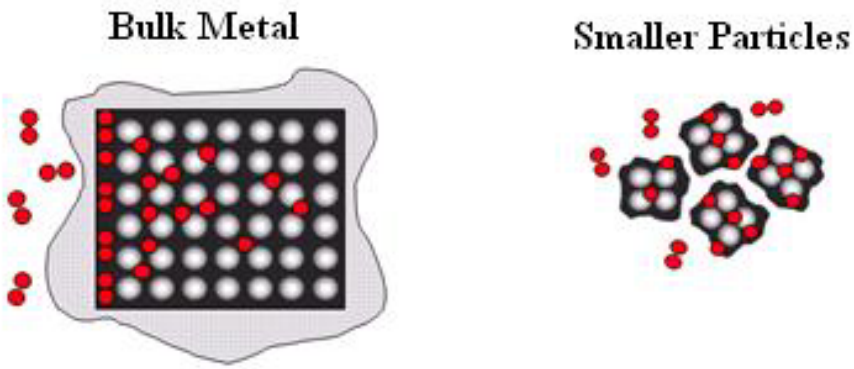

Figure 2.10. Bulk Metal versus Smaller Particles

Producing smaller magnesium particles via ball milling improves both the morphology of the powders and the surface activity for hydrogenation. When a smaller structure is combined with surface modification, the result is a dramatic

improvement of the sorption kinetics [44]. However, in order to have an economically feasible hydrogen storage system, a safe, efficient and low cost method should be developed for material processing. Also, an increase in the particles size as a result of sintering during H_2 absorption/desorption cycles should be avoided.

2.8 Alloying Magnesium with Different Metals

In 2005, Au et al confirmed that mechanical alloying reduces particle sizes and introduces mechanical stress causing an improvement in the hydrogenation kinetics of the magnesium based materials even at low temperatures, but high temperatures are still needed to release the absorbed hydrogen from the materials [3].

Since each alloy has different performance characteristics (hydrogen absorption capacity, charge/discharge kinetics, operating range of temperature and pressure, heat of reaction, and cycling capabilities), multicomponent hydrogen storage systems can be tailored to have a better hydrogenation/dehydrogenation kinetics, lower desorption temperatures and higher hydrogen storage capacities. Therefore alloys offer a great potential for practical hydrogen storage systems [31].

An intermetallic compound RM_n (where R = rare earth and M = a late transition or main group metal) usually shows intermediate hydriding and dehydriding characteristics between those of two elements R and M which, in general, causes a reversible behavior near atmospheric pressure at room temperature. RM_n compounds are usually classified by families according to their stoichiometry n. Various storage capacities hydrogenation/dehydrogenation characteristics are obtained depending on the value of n. The most studied values today are equal to n = 1/2; 1, 2 and 5 [26].

Figure 2.11 shows that the mass capacity strongly depends on the molar mass of the compounds and using lighter elements cause an improvement on the storage capacity. However, composition has no significant effect on the volume capacity.

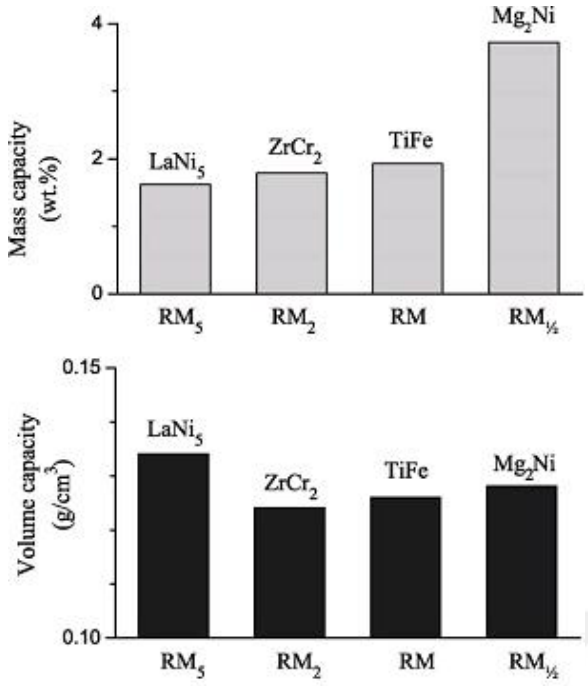

Figure 2.11. Comparison Between Mass and Volume Capacities of Various RM_n-Type Compounds

Figure 2.11 also indicates that most compounds have hydrogen densities twice larger than of liquid hydrogen (also easier to handle under 1.7 bar of equilibrium pressure at room temperature) [26].

Transition metals are known to significantly improve the catalytic activity on the absorption and desorption of hydrogen molecule, and as a result, increases the hydriding/dehydriding rates [45].

At ambient temperatures, Mg-$LaNi_5$ composite systems have the potential to be developed as rapid discharge hydrogen storage materials. Since $LaNi_5$ has fast hydriding/dehydriding kinetics with a low hydrogen storage capacity and Mg has high capacity among other known metal hydrides with slow hydrogen desorption rates (even at high temperatures like 300°C), it is aimed to develop a Mg-$LaNi_5$ system which combines the advantages of the both materials and offsets their disadvantages. If the $LaNi_5$ phase is distributed homogeneously on the magnesium matrix, hydro-

gen storage capacity at room temperature might be increased further [3]. In 2005, Au showed that adding $LaNi_5$ in magnesium improves the hydrogen storage performance at room temperatures. The nano/amorphous composite material Mg (80%) -$LaNi_5$ (20%) absorbed and desorbed 1.9 wt. % and 1.7 wt. % hydrogen at 25°C respectively. The amount of hydrogen absorbed and desorbed increased by increasing temperature. As a result, the nano/amorphous composite structure improved the hydriding/dehydriding kinetics, reduced hydriding temperature and enhanced hydrogen storage capacity of magnesium based materials. Adding lanthanum into Mg-Ni nano/amorphous composite materials reduced the hydriding and dehydriding temperature from 200°C to 25°C. This indicates that the thermodynamic stability of Mg-Ni nano/amorphous composite materials can be reduced by additives such as La or other effective elements [3]. In 2008, Tanaka showed that a Mg-rich alloy containing $\sim$ 10 wt. % Ni and $\sim$ 5 wt. % La exhibits excellent reaction kinetics, desorbing $\sim$ 5 wt. % hydrogen at a temperature as low as 200°C in a moderate time period [38].

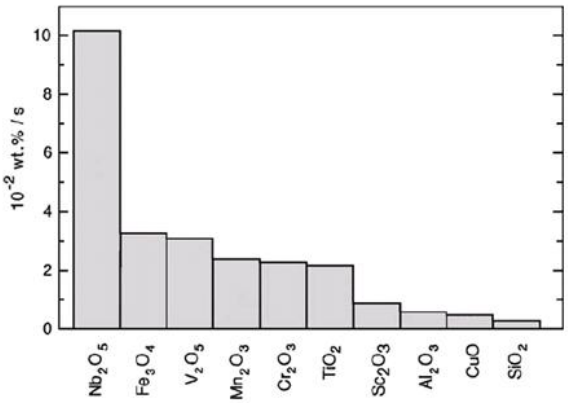

Figure 2.12. Comparison of the Desorption Rates of MgH_2 with Different Metal Oxide Catalysts

Nb hydride plays a deterministic role in improving the absorption/desorption kinetics of MgH_2 [25]. Nb_2O_5 is the most effective catalyst for the hydrogen absorption/desorption reactions of Mg known so far (see Figure 2.12). The high-performance catalytic effect of Nb_2O_5 is also observed at lower temperatures [4].

The goal of this thesis is to prepare and test a new magnesium-based metal hydride that has high hydrogen sorption and desorption rates at lower temperatures and high hydrogen storage capacity. The catalytic effect of Nb_2O_5 is used to increase the desorption rate of magnesium hydride and $LaNi_5$ is chosen for its fast hydriding/dehydriding kinetics. The new sorbent, MgH_2-$LaNi_5$-Nb_2O_5, is developed to combine the advantages of those materials and minimize their disadvantages.

CHAPTER 3
EXPERIMENTAL SETUP, PROCEDURE, AND MATERIAL PREPARATION

3.1 Experimental Setup

The main idea of our experimental setup is to test the capacity of the hydrogen storage materials in both charging and discharging processes. Usually the capacity is measured in terms of hydrogen to storing material weight percent (H/M wt. %).

The absorption/desorption capacity of the sample and the rate of absorption/desorption were measured using a manual controlled Sievert apparatus equipped with computer data acquisition (see Figure 3.1).

The setup is composed of the following parts;

i. Hydrogen and helium cylinders and pressure regulators
ii. VCR high pressure valves to control hydrogen flow through the setup
iii. Micro compressor to post hydrogen pressure in case of hydrogen pressure in the hydrogen cylinder less than the pressure required for high pressure storing materials
iv. Stainless steel chasteners to store hydrogen for absorption/desorption test
v. High pressure and low pressure (vacuum) transducer for measuring the high pressure and vacuum pressure of the setup
vi. Sample chamber for the material to be tested
vii. Electrical heater to apply heat in the sample chamber
viii. Temperature controller to control and monitor the temperature of the sample chamber

ix. Vacuum pump

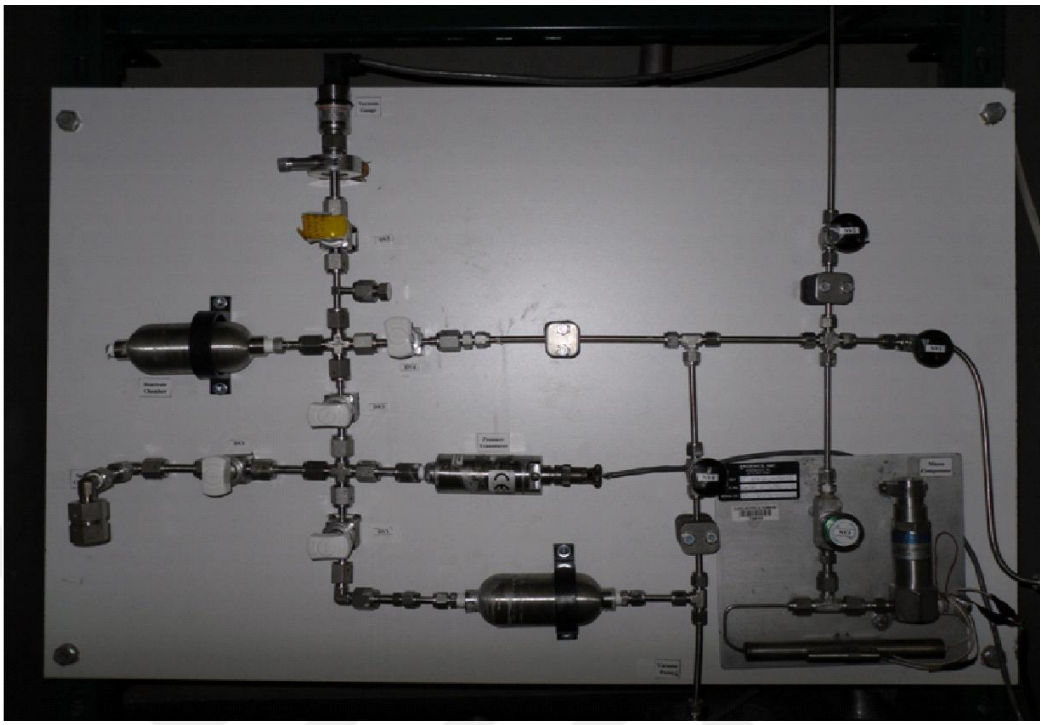

Figure 3.1. Hydrogen Absorption/Desorption Experiment Apparatus

As can be seen from Figure 3.2, the region between DV1, DV2 and DV3 including the pressure transducer is called the high pressure (HP) zone. High pressure zone is the part where hydrogen is introduced first. Sample chamber (SC) zone is separated from the high pressure zone by the valve DV2. After reaching a constant pressure reading at high pressure zone, DV2 is opened and the hydrogen gas is introduced to the sample chamber zone. The steady state pressure reading at this step is called the equilibrium pressure.

The high pressure zone and the sample chamber zone are the main parts of the experimental setup used during absorption and desorption experiments. The calculations are performed based on the difference between the initial pressure at high pressure zone and the steady state pressure of high pressure zone and the sample chamber zone combined.

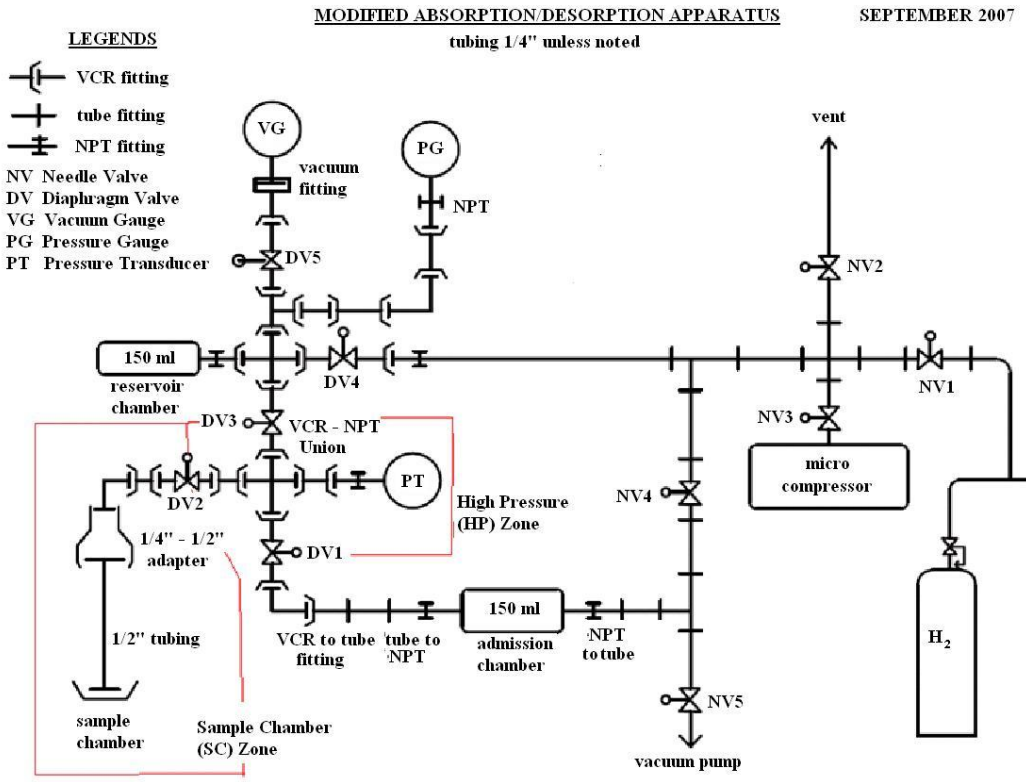

Figure 3.2. Schematic of Hydrogen Absorption/Desorption Experiment Apparatus

3.2 Sample Preparation Procedure

MgH_2, Nb_2O_5 and $LaNi_5$ were purchased from Sigma-Aldrich, Inc. The average purity and particle size were 99.5 % and 50 μm, respectively. 7.27 g MgH_2, 0.73 g Nb_2O_5 and 2 g $LaNi_5$ were weighed and put into a 45 mL zirconia ceramic vial. The diameter and length of the vial were 6.35 cm and 6.8 cm. Two 12.7 mm diameter zirconia ceramic balls from SPEX SamplePrep 8005 Vial Set were put into the vial. And the vial was loaded in a SPEX-8000^{TM} high energy ball mill. Every 90 minutes, the vial was taken out for scraping the material adhering on the wall. In this work, the ball-milling process took about 6 hours. To avoid any possible oxidation, the powder was handled and processed in an argon-filled glove box near atmospheric pressure.

3.3 Particle Size Determination Procedure

Sample particle size was measured by laser diffraction particle sizing technique. In this technique, particles passing through a laser beam scatter light at an angle that is directly related to their size. As the particle size decreases, the observed scattering angle increases logarithmically. The observed scattering intensity is also dependent on particle sizes and diminishes, to a good approximation, in relation to the particle's cross-sectional area. Large particles therefore scatter light at narrow angles with high intensity, whereas small particles scatter light at wider angles but with low intensity.

The primary measurement that has to be carried out within a laser diffraction system is the capture of the light scattering data from the particles under study. A typical system consists of (see Figure 3.3):

- *A laser*, to provide a source of coherent, intense light of fixed wavelength
- *A sample presentation system* to ensure that the material under test passes through the laser beam as a homogenous stream of particles in a known, reproducible state of dispersion
- *A series of detectors* which are used to measure the light pattern produced over a wide range of angles

The size range accessible during the measurement is directly related to the angular range of scattering measurement. Modern instruments make measurements from around 0.02 degrees through to 135 degrees. A logarithmic detector sequence, where the detectors are grouped closely together at small angles and more widely spaced at wide angles, yields the optimum sensitivity. Finally, the detector sequence is generally set up such that equal volumes of particles of different sizes produce a similar measured signal. This requires the size of the detectors to be increased as the measured scattering angle increases.

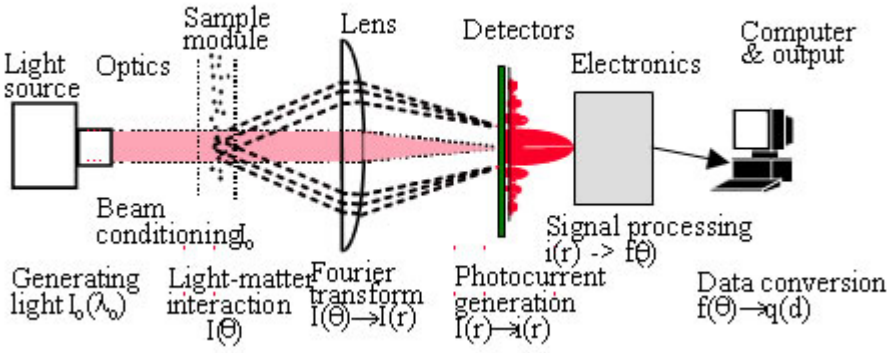

Figure 3.3. Schematic of Laser Diffraction Particle Sizing

After the ball-milling procedure, SRA150 by Microtrac, USA was used to measure the sample size of the new composite material. The particle size determination procedure started with dispersing and circulating the particles in water through the laser beam with a pump. The scattered laser was then collected by detectors and the software interpreted the average particle size of the new composite material around 5 - 7 μm.

3.4 Experimental Procedures

Hydrogen storage capacity is tested for both charging and discharging at different equilibrium pressures. Each experimental run is done at constant temperature at different pressure. At each equilibrium pressure, there is a certain storage capacity for the storing material. The plot which shows the equilibrium pressure with the hydrogen to material weight percent (H/M wt. %) at constant temperature gives a curve called Pressure Composition Isotherm (PCI).

The hydrogen absorption experiments were conducted around 500 psi and the hydrogen desorption experiments were conducted at atmospheric pressure at different temperatures. The pressure composition-isotherms (PCI) were measured by an automatic Sievert volumetric analysis instrument equipped with a computer data

acquisition.

3.4.1 Manifold Drydown Procedure.

It is a good practice to perform a drydown/purge procedure to remove particles/contaminants in the system after initial construction and during operation (especially when the system is opened to atmosphere e.g. during a sample chamber change out). There are two ways of accomplishing drydown:

- High flow of an inert gas through the system
- Pressure/vacuum purge cycling

Since our system has several deadlegs, it is needed to perform both procedures to effectively purge down all sections of the manifold. Purging can be done with or without heating the manifold. Heating to 105°C helps drive off moisture and organics on the tube/fitting surface. The sample chamber might be heated to the temperature that will be used to activate the metal hydride in order to drive off any contaminants that could vaporize at that temperature. Here is a possible purge procedure (see Figure 3.2):

i. NV1 is closed and He delivery pressure is set to 60 psig.

ii. NV5 is opened and vacuum pump is started.

iii. NV4 and DV5 are closed; DV3, DV4 and NV1 are opened to allow manifold to pressurize.

iv. NV1 is closed and NV4 is opened to allow pressurized He to evacuate until vacuum stabilizes.

v. NV4 is closed and NV1 is opened to pressurize the system.

vi. Steps iv and v are repeated, twenty to thirty times.

3.4.2 Sorbent Activation Procedure.

After ball-milling, the new composite material has to be activated in order to prepare it for the first absorption experiment. Also, it is beneficial to repeat the activation procedure before each absorption experiment. It should be noticed that each storage material as its own activation procedure, but generally an activated material should be kept away from oxygen in order to avoid the formation of metal oxides.

i. About 3.0 g of the material is weighed.

ii. The material is placed in the sample chamber, usually to the furthermost end of the chamber and a 2 μm stainless steel mesh mounted at the top of sample chaber is used to keep the metal hydride in the sample chamber during vacuum.

iii. All valves are opened except NV1 and NV2 (vent valve). The vacuum pump is turned on and the experimental setup is evacuated (typically reaches about -12.2 psi).

iv. Heat is applied to the sample chamber up to 400 °C while vacuum is being applied, approximate time for heating is 15 minutes. The coming two steps should be done immediately.

v. NV4, NV5, DV1, DV2 and DV5 are closed and the vacuum pump is turned off.

vi. NV1 is opened and the system is pressurized with approx. 500 psi hydrogen, then DV3 and DV4 are closed. DV2 is opened and the sample is allowed to cool down to room temperature. Internal pressure decreases due to the hydrogen absorption indicating sufficient activation to begin PCT measurement, this typically takes 30 minutes.

vii. Once pressure stabilizes, indicating hydrogen activation/saturation, the vacuum pump is turned on and NV5, DV1 and DV2 are opened.

viii. Heat is applied to the sample chamber (typically 400 °C) to get the material fully desorbed. Vacuum is applied up to -12.2 psi.

ix. Once the sample is fully desorbed, NV1, NV5, DV1 and DV2 are closed and the vacuum pump is turned off.

The sample can then be used for the Pressure Composition Isotherm (PCI) measurement at the desired temperature.

3.4.3 Charging Procedure.

After sample preparation, the sample should be under vacuum with all the valves closed. If the run is a second or higher (3^{rd}, 4^{th} etc) run, the setup must be evacuated before starting. To evacuate the setup, the vacuum pump should be turned on with all valves fully opened except NV1 and NV2. When the pressure reaches about -12.2 psi, the valves can be closed one by one: NV5, NV4, DV1, DV2, DV3, DV4 and DV5.

For charging, the following steps are done:

i. Hydrogen pressure is adjusted from the hydrogen cylinder pressure regulator to the required pressure.

ii. NV1 is opened.

iii. DV3 and DV4 are opened until the pressure reading is established and then DV3 and DV4 are closed.

iv. The pressure reading is taken from high pressure transducer (the number of moles entered the high pressure zone is calculated by using gas law).

v. DV2 is opened. Sharp pressure decrease due to the pressure difference between the high pressure zone and sample chamber zone is observed. Then, the hydrogen absorption starts which leads to a gradually decrease in the pressure.

vi. When the pressure reading reaches a constant value, the reading is taken again using the high pressure transducer (the number of moles at the equilibrium pressure in the high pressure and sample chamber zones is calculated by using gas law).

vii. DV2 is closed.

viii. Steps iii-vii are repeated until getting enough points for constructing an isotherm (about 15-20 points are usually enough, it also depends on whether the point is at the edges or in the middle of the curve).

ix. For the last run, DV2 and NV1 are closed and no more hydrogen is added.

3.4.4 Discharging Procedure.

After charging the sample with hydrogen, the discharging experiments are done immediately. There will be hydrogen in the high pressure assembly with all the valves are closed.

For discharging, the following steps are done:

i. The pressure reading is taken from the high pressure transducer.

ii. Hydrogen pressure in the high pressure zone is reduced by partially opening DV1, and then DV1 is closed.

iii. The high pressure transducer reading is taken again. This is the high pressure zone reading.

iv. DV2 is opened. Sharp pressure increase due to the pressure difference between the sample chamber and high pressure zone is observed and the pressure gradually increases until it reaches a constant value.

v. The pressure reading is taken from the high pressure transducer, the pressure reading will be higher than the one taken in step 3 because of hydrogen desorption.

vi. DV2 is closed.

vii. Steps ii-vi are repeated. The last run is performed when the starting equilibrium pressure from charging procedure is reached.

CHAPTER 4
ANALYSIS OF THE EXPERIMENTAL DATA

The goal of this chapter is to develop a procedure to calculate the number of moles adsorbed/desorbed during charging and discharging steps using our pressure data.

4.1 Assumptions

During the course of our experiments, several assumptions were made in order to simplify the calculations.

While calculating the volume occupied by the sample material, the bulk density was used and the porosity of the sorbent particles was ignored. Therefore, the sorbent was considered as a black box with a density of 1.37 cm^3. This amount was taken into account while calculating the amount of hydrogen absorbed/desorbed in the sample.

The amount of hydrogen adsorbed/desorbed depends on the difference between the high and equilibrium pressures. Since the compressibility factor of hydrogen is about 1 within the operating temperature and pressure range used during the experiments; ideal gas assumption was used to calculate the number of moles of hydrogen absorbed/desorbed.

As shown and mentioned in experimental setup and experimental procedures sections; the high pressure zone and the sample champer zone are the main parts of the experimental setup that we focused on. During experiments which took place at temperatures higher than room temperature (100, 200 and 300 °C), sample chamber was the only part heated up to those temperatures. Because of the lack of a better heating system that would heat up the entire system to the desired temperature including the hydrogen source or a better temperature sensor which would monitor

the temperature at different parts of the setup; sample chamber zone was assumed to be at experimental temperature and high pressure zone was assumed to be at room temperature during the absorption and desorption experiments.

4.2 Gas Leak

Leak test is performed at different pressures for the purpose of incorporating error in the quantity of hydrogen loss during the experiments. Several leak tests are performed at 20°C (room temperature), 100°C, 200°C and 300°C and 100, 200, 300, 400 and 500 psig.

Using the volume calculations and ideal gas law, the leak rate is determined in terms of mol/min. And the total hydrogen loss during an absorption (or desorption) cycle is taken into account while calculating the absorption (or desorption) capacity of the material.

4.3 Number of Moles of Hydrogen Absorbed During Charging

Table 4.1 and Table 4.2 show the high pressure zone and sample chamber zone volume calculations. Volume of the high pressure zone is 6.43 cm^3, volume of the sample chamber zone is 18.50 cm^3. Combined, high pressure and sample chamber zones constitute the equilibrium zone with a volume of 24.93 cm^3.

Table 4.1. High Pressure Zone Volume Calculation

Unit Name	Unit Code	No	Length (cm)	Diameter (cm)	Volume	Total Volume
Union Cross	SS-4-VCR-CS	1	2.72	0.46	1.81	1.81
Rotating Female Union	SS-4-WVCR-6-DF	2	4.34	0.46	0.72	1.44
Valve	6LVV-DPHFR4	2	3.53	0.46	0.59	1.17
Valve	6LVV-DPHVR4	1	2.92	0.46	0.49	0.49
Pressure Transducer						1.52

Table 4.2. Sample Chamber Zone Volume Calculation

Unit Name	Unit Code	No	Length (cm)	Diameter (cm)	Vol.	Total Vol.
Union Elbow	SS-4-VCR-9	2	2.72	0.46	0.90	1.81
Rotating Female Union	SS-4-WVCR-6-DF	2	4.34	0.46	0.72	1.44
Female Reducing Union	SS-8-VCR-6-DF-4	1	0.89	0.64	0.29	0.29
Valve	6LVV-DPHVR4	1	2.92	0.46	0.49	0.49
1/2 inch tube						14.47

The following procedure was used to calculate the number of moles of hydrogen stored in the storing sample during charging;

i. The number of moles initially in the high pressure zone is calculated by using the ideal gas law;

$$PV = nZRT \tag{4.1}$$

Where P is the pressure reading from step iv in the charging procedure, V is the volume of high pressure zone, n is the number of moles initially in the high pressure zone, Z is the compressibility factor (which will be assumed as 1), R is the gas constant and T is the temperature.

ii. The number of moles in the high pressure and sample chamber zone is calculated by using the ideal gas law and the pressure reading from step vi in the charging procedure. The volume now includes the high pressure zone (V_{HP}) and sample chamber zone (V_{SC}).

iii. The difference between moles in steps i and ii is the number of moles adsorbed. This number is multiplied by the molecular weight of hydrogen to get the hydrogen weight and divided by the sample weight to get the weight percent (H/M wt. %).

iv. This (H/M wt. %) is plotted with the equilibrium pressure, pressure taken in step vi in the charging procedure to construct the Pressure Composition Isotherm chart.

4.4 Number of Moles of Hydrogen Desorbed During Discharging

To calculate the number of moles of hydrogen released from the storing sample during discharging, the following procedure was used;

i. The number of moles initially in the high pressure zone is calculated by using the ideal gas law and the pressure reading from step iii in the discharging procedure and only high pressure zone volume.

ii. The number of moles in the high pressure and sample chamber zone is calculated by using the ideal gas law and the pressure reading from step v in the discharging procedure. The volume now includes the high pressure zone (V_{HP}) and sample chamber zone (V_{SC}).

iii. The difference between moles in steps i and ii is the number of moles desorbed. This number is multiplied by the molecular weight of hydrogen to get the hydrogen weight and divided by the sample weight to get the weight percent (H/M wt. %).

iv. This (H/M wt. %) is plotted with the equilibrium pressure, pressure taken in step iii in the discharging procedure to construct the Pressure Composition Isotherm chart.

CHAPTER 5
RESULTS AND DISCUSSION

This chapter covers the results of the adsorption and desorption experiments at various temperatures by using the assumptions and calculation techniques mentioned in the previous chapter.

Section 5.1 shows the experimental setup leak test results. By using the hydrogen leak rate mentioned in Section 5.1, the amount of hydrogen lost during charging/discharging experiments was estimated and taken into account when calculating the amount of hydrogen adsorbed/desorbed. By taking the hydrogen leak rate into account, more precise results were obtained without overestimating the adsorption capacity or underestimating the amount of hydrogen desorbed.

Section 5.2 explains the results of hydrogen adsorption and desorption experiments at 300, 200, 100 and 20°C, respectively. The hydrogen storage capacity and the amount of hydrogen desorbed are explained using wt.% and those results are compared to the data from the literature for each temperature. Also, the adsorption and desorption rates are calculated based on the amount of hydrogen adsorbed/desorbed (in wt.%). The amount of time to reach 80% of the capacity was used to determine the hydrogen adsorption/desorption rates in wt.%/s. The hydrogen adsorption/desorption rates are also compared to the data from the literature and presented in each section for different temperatures.

5.1 Gas Leak Test Results

Figure 5.1 shows that the experimental setup has a slight leak, which depends on the operating pressure and the operating temperature. Overall, the highest leak rate was observed at 500 psig and 300°C which was 0.18 psia per min. An average absorption experiment lasted 8 hours and the total amount of hydrogen loss was

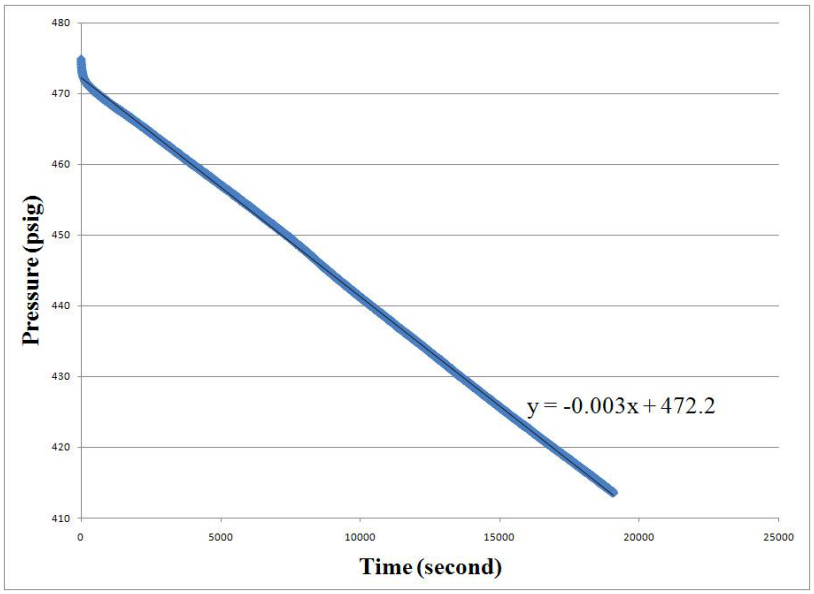

Figure 5.1. Leak Test Result at 300°C

approximately 0.012 g. The amount of hydrogen loss was around 6 % of the hydrogen absorbed at 500 psig and 300°C. At 500 psig and 20°C, about 0.007 grams of hydrogen was lost during an 8 hour absorption experiment which was approximately 8 % of the total amount of hydrogen absorbed. The lowest leak rate was observed at 100 psig and 20°C which resulted a hydrogen loss of 0.0008 g during an 8 hour experiment. On average, 6 - 8 % of the hydrogen absorbed/desorbed was lost during the course of the experiments. This amount was taken into account while calculating the hydrogen absorption/desorption capacity of the sample material.

5.2 Effect of Temperature on the Absorption/Desorption Capacity and Rate

Figure 5.2 and Figure 5.3 show the effect of temperature on hydrogen storage capacity and rate of the sample. Both figures indicate that the hydrogen storage capacity and rate increase with increasing temperature. From Figure 5.2, it can be seen that it was not possible to release all of the absorbed hydrogen during desorption. On average, 85 % of the absorbed hydrogen could be released successfully during

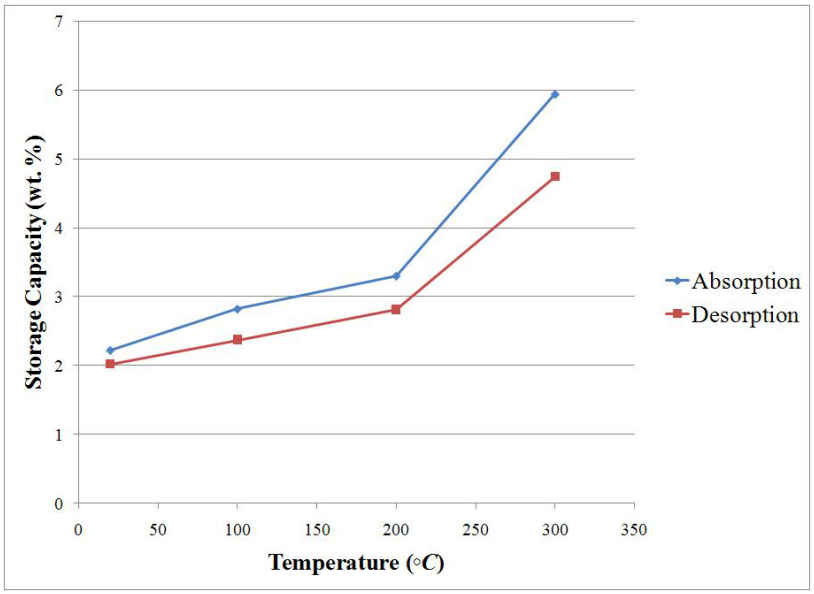

Figure 5.2. The Effect of Temperature on Hydrogen Storage Capacity of the Sorbent

desorption experiments. However, the percentage of the hydrogen released during desorption decreases with increasing temperature. For instance, 91 % of the hydrogen could be released successfully at 20°C while 86 % did at 100°C, 84 % did at 200°C and 80% at 300°C. Similarly, Figure 5.3 shows that the absorption rate is higher than the desorption rate at all temperature ranges. However, the difference between the absorption and desorption rates can be seen more prominently at higher temperatures. Although our sorbent's absorption/desorption rates exceeded the ones from the literature, Figure 5.3 indicates that our sorbent's hydrogen storage rates were lower than 0.005 wt.%/s except at 300°C. The dramatic difference between absorption/desorption rates at 200°C and 300°C can be explained by magnesium hydrides' superior hydrogen storage rates at high temperatures.

To form MgH_2, first H_2 needs to overcome an activation barrier for dissociation. The heat of formation of H_2 is - 286 kJ/mol. Therefore, 286 kJ/mol of energy is needed to break the bond between the hydrogen atoms of the hydrogen molecule. On the other hand, the heat of formation of MgH_2 is -78 kJ/mol. As a result, the

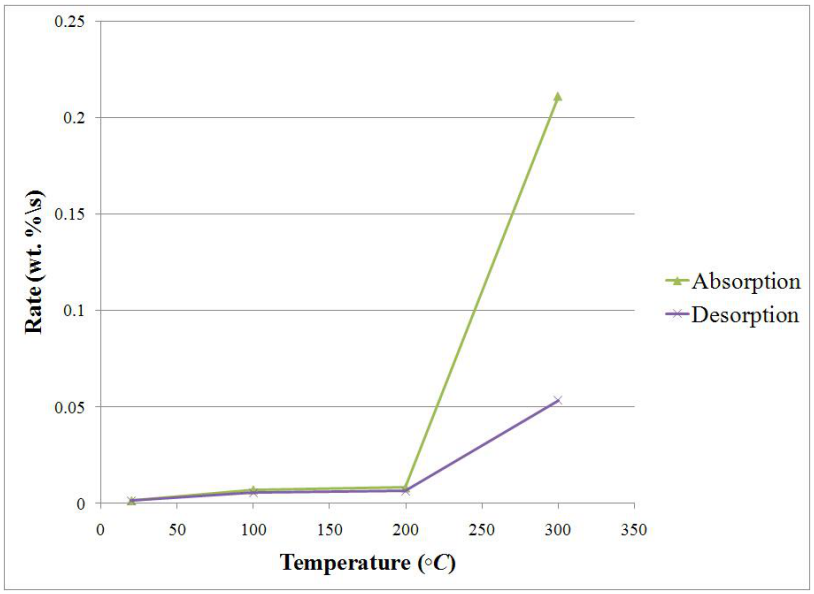

Figure 5.3. The Effect of Temperature on Hydrogen Storage Rate of the Sorbent

process of breaking the bond between the hydrogen atoms and forming a magnesium hydride is highly endothermic because of the high energy needs of dissociation of hydrogen (around 208 kJ/mol of energy needed in total). Also, the heat of formation of $LaNi_5H_6$ is -285 kJ/mol. Since 3 moles of H_2 needs to be dissociated in order to form one mole of $LaNi_5H_6$, the dissociation reaction of hydrogen molecule and formation reaction of $LaNi_5H_6$ combined is highly endothermic. When the heat of formation of H_2, MgH_2 and $LaNi_5$ taken into account; it could be seen that the dissociation reaction of H_2 and formation reactions of MgH_2 and $LaNi_5H_6$ together is highly endothermic which means the hydrogen absorption reactions of both hydrides are favored at higher temperatures. Similarly, the desorption reactions are highly endothermic and favored at higher temperatures. Based on the heat of reaction data provided so far and from figures 5.2 and 5.3, it can be concluded that both absorption and desorption reactions would be more favorable at 400°C compared to 300°C.

5.2.1 Experimental Results at 300°C.

Figure 5.4 shows both the absorption and desorption pressure composition

Table 5.1. Summary of the Experimental Results Compared to the Literature at 300°C

Average	Our Data MgH_2-$LaNi_5$-Nb_2O_5 (approx. 500 psi)	Au (2005) MgH_2-20 wt.% $LaNi_5$ (approx. 435 psi)	Barkhordarian (2003) MgH_2-7.3 wt.% Nb_2O_5 (approx. 421 psi)	Wu (2006) MgH_2 (approx. 428 psi)
	HYDROGEN STORAGE CAPACITY (AT 300°C) (wt.%)			
Absorption	5.94	5.5	4.9	5.5
Desorption	4.74	4.2	4.7	4 (350°C)
	HYDROGEN STORAGE RATE (AT 300°C) (wt.%/s)			
Absorption	0.211	0.0183	0.185	0.00233
Desorption	0.0532	0.00175	0.0492	0.0011 (350°C)

isotherms of MgH_2-$LaNi_5$-Nb_2O_5 composite material at 300°C. Table 5.1 shows that at around 500 psi and 300°C, MgH_2-$LaNi_5$-Nb_2O_5 composite material absorbed about 5.94 wt.% hydrogen with a rate of 0.211 wt. %/s and desorbed about 4.74 wt.% hydrogen with a rate of 0.0532 wt.%/s.

The absorption/desorption capacity of MgH_2-$LaNi_5$-Nb_2O_5 composite material is higher than the absorption and desorption capacity of MgH_2-$LaNi_5$. According to Au's work in 2005, MgH_2-$LaNi_5$ composite material gave a hydrogen storage capacity of 5.5 wt.% with a rate of 0.0183 wt.%/s and the desorption capacity of the material was 4.2 wt.% with a rate of 0.00175 wt.%/s at 300°C and around 435 psi [3]. Both MgH_2-$LaNi_5$-Nb_2O_5 and MgH_2-$LaNi_5$ had 20 wt.% $LaNi_5$. Therefore, removing 7.3 wt.% of the MgH_2 and replacing it by Nb_2O_5 not only improved the absorption and desorption capacity, but also increased the rate of absorption/desorption rates of the composite material. The difference in absorption and desorption rates is even more clear, 30 times faster desorption and 10 times faster absorption were observed when 7.3 wt.% of the MgH_2 was replaced by Nb_2O_5.

Our results showed that using both $LaNi_5$ and Nb_2O_5 increased both the absorption capacity and the rate. Using $LaNi_5$ in addition to MgH_2-Nb_2O_5 had a positive effect on hydrogen storage capacity while using Nb_2O_5 in addition to MgH_2-$LaNi_5$ significantly increased the absorption rate. Compared to the absorption capacity and rate data of MgH_2 currently available in the literature, our novel material had a significantly higher absorption rate. Using $LaNi_5$-Nb_2O_5 in addition to MgH_2 also increased the absorption capacity. However, the difference in absorption rate data was much more obvious, the absorption rate of our novel material was at least 75 times higher than the data currently available in the literature.

Although the difference between the desorption capacities is pretty small (see Table 5.1), adding $LaNi_5$ and Nb_2O_5 significantly increased the desorption rate. The effect of Nb_2O_5 on desorption rate can be clearly seen from this data. Literature showed that using only MgH_2 caused a much lower desorption capacity, even at higher temperatures. And our novel material had a much higher desorption which showed that adding $LaNi_5$ and Nb_2O_5 had a significant effect on both desorption rate and capacity.

When the absorption/desorption capacity and rate of MgH_2-$LaNi_5$-Nb_2O_5 are compared to the data of MgH_2 in the literature, it can be seen that the new composite material has a higher absorption/desorption capacity and rate [42], [6], [21].

5.2.2 Experimental Results at 200°C.

The absorption and desorption pressure composition isotherms of MgH_2-$LaNi_5$-Nb_2O_5 composite material at 200°C are shown in Figure 5.5. Table 5.2 indicates that MgH_2-$LaNi_5$-Nb_2O_5 composite material absorbed about 3.30 wt.% hydrogen with a rate of 0.00827 wt. %/s and desorbed about 2.81 wt.% hydrogen with a rate of

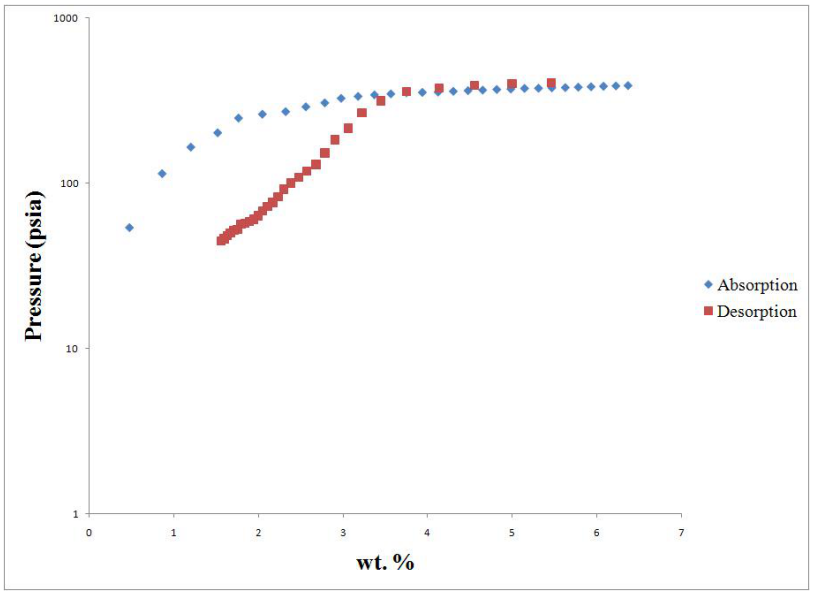

Figure 5.4. Absorption and Desorption PCI Curves at 300°C

0.00635 wt.%/s at around 500 psi and 200°C.

Compared to MgH_2-$LaNi_5$, MgH_2-$LaNi_5$-Nb_2O_5 composite material has higher absorption/desorption capacity and rate. In 2005, Au showed that MgH_2-$LaNi_5$ composite material has hydrogen storage capacity of 2.9 wt.% with a rate of 0.00242 wt.%/s and desorption capacity of the material was 2.3 wt.% with a rate of 0.000958 wt.%/s at 200°C and around 435 psi [3]. As mentioned before, both MgH_2-$LaNi_5$-Nb_2O_5 and MgH_2-$LaNi_5$ had 20 wt.% $LaNi_5$. Again, removing 7.3 wt.% of the MgH_2 and replacing it by Nb_2O_5 not only improved the absorption and desorption capacity, but also increased the rate of absorption/desorption rates of the composite material. The difference in absorption and desorption rates is even more clear, 4 times faster desorption and 7 times faster absorption were observed when 7.3 wt.% of the MgH_2 was replaced by Nb_2O_5.

When the absorption/desorption capacity and rate of MgH_2-$LaNi_5$-Nb_2O_5 are compared to the data of MgH_2 in the literature, it can be seen that the new composite material has a higher absorption/desorption capacity and rate than MgH_2

Table 5.2. Summary of the Experimental Results Compared to the Literature at 200°C

Average	Our Data MgH_2-$LaNi_5$-Nb_2O_5 (approx. 500 psi)	Au (2005) MgH_2-20 wt.% $LaNi_5$ (approx. 435 psi)	Wu (2006) MgH_2 (approx. 428 psi)
	HYDROGEN STORAGE CAPACITY (AT 200°C) (wt.%)		
Absorption	3.3	2.9	2.5
Desorption	2.81	2.3	1.7
	HYDROGEN STORAGE RATE (AT 200°C) (wt.%/s)		
Absorption	0.00827	0.00242	0.000347
Desorption	0.00635	0.000958	0.000236

alone [42]. The absorption/desorption rate of the new composite material is about 25 times higher than MgH_2.

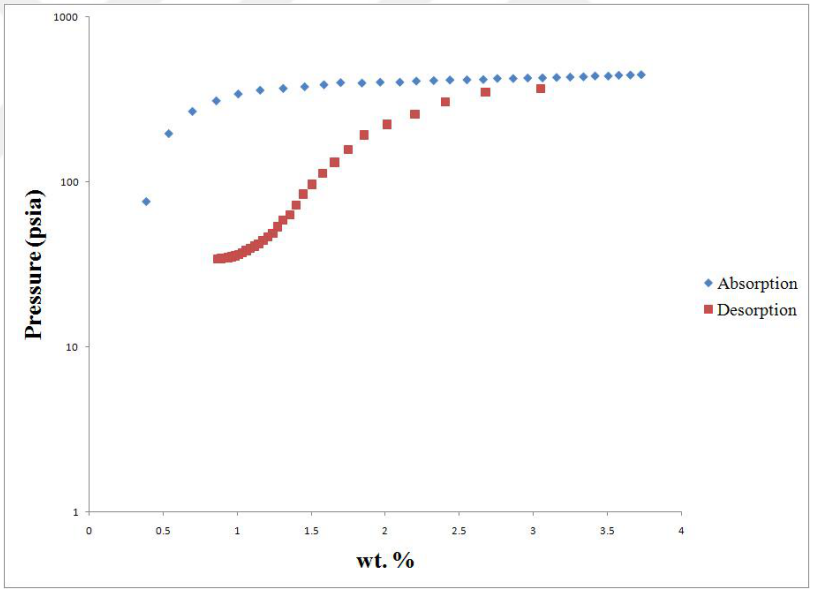

Figure 5.5. Absorption and Desorption PCI Curves at 200°C

5.2.3 Experimental Results at 100°C.

Figure 5.6 shows both the absorption and desorption pressure composition isotherms of MgH_2-$LaNi_5$-Nb_2O_5 composite material at 100°C. And from Table 5.3,

Table 5.3. Summary of the Experimental Results Compared to the Literature at 100°C

Average	Our Data MgH_2-$LaNi_5$-Nb_2O_5 (approx. 500 psi)	Au (2005) MgH_2-20 wt.% $LaNi_5$ (approx. 435 psi)	Liu (2006) MgH_2 (approx. 1000 psi)
	HYDROGEN STORAGE CAPACITY (AT 100°C) (wt.%)		
Absorption	2.82	2.4	1.5
Desorption	2.37	1.9	0.9
	HYDROGEN STORAGE RATE (AT 100°C) (wt.%/s)		
Absorption	0.00718	0.000333	0.0002
Desorption	0.0054	0.000264	0.000125

it can be seen that MgH_2-$LaNi_5$-Nb_2O_5 composite material absorbed about 2.82 wt.% hydrogen with a rate of 0.00718 wt. %/s and desorbed about 2.37 wt.% hydrogen with a rate of 0.0054 wt.%/s at around 500 psi and 100°C.

Compared to MgH_2-$LaNi_5$, MgH_2-$LaNi_5$-Nb_2O_5 composite material has higher absorption/desorption capacity and rate. In 2005, Au showed that MgH_2-$LaNi_5$ composite material has hydrogen storage capacity of 2.4 wt.% with a rate of 0.000333 wt.%/s and desorption capacity of the material was 1.9 wt.% with a rate of 0.000264 wt.%/s at 100°C and around 435 psi [3]. As mentioned before, both MgH_2-$LaNi_5$-Nb_2O_5 and MgH_2-$LaNi_5$ had 20 wt.% $LaNi_5$. Again, removing 7.3 wt.% of the MgH_2 and replacing it by Nb_2O_5 not only improved the absorption and desorption capacity, but also increased the rate of absorption/desorption rates of the composite material. The difference in absorption and desorption rates is even more clear, almost 25 times faster absorption and desorption were observed when 7.3 wt.% of the MgH_2 was replaced by Nb_2O_5.

When the absorption/desorption capacity and rate of MgH_2-$LaNi_5$-Nb_2O_5 are compared to the data of MgH_2 in the literature, it can be seen that the new

composite material has a higher absorption/desorption capacity and rate than MgH_2 alone [27]. In 2006, Liu et al showed that MgH_2 has hydrogen storage capacity of 1.5 wt.% with a rate of 0.0002 wt.%/s and desorption capacity of the material was 0.9 wt.% with a rate of 0.000125 wt.%/s at 100°C and around 1000 psi. Although the pressure used was two times higher than this work, adding $LaNi_5$ and Nb_2O_5 to MgH_2 significantly increased the hydrogen absorption/desorption capacity and rate. The new composite material worked a lot better than MgH_2 with 2 - 3 times higher absorption and desorption capacity and 40 times higher absorption/desorption rate at lower pressures.

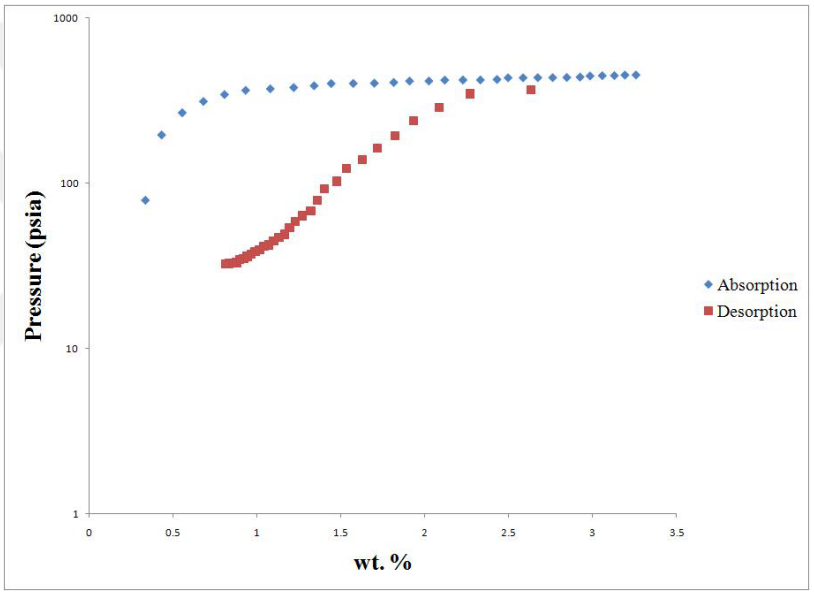

Figure 5.6. Absorption and Desorption PCI Curves at 100°C

5.2.4 Experimental Results at 20°C.

The absorption and desorption pressure composition isotherms of MgH_2-$LaNi_5$-Nb_2O_5 composite material at 20°C are shown in Figure 5.7. Table 5.4 shows that MgH_2-$LaNi_5$-Nb_2O_5 composite material absorbed about 2.22 wt.% hydrogen with a rate of 0.00152 wt. %/s and desorbed about 2.02 wt.% hydrogen with a rate of 0.00127 wt.%/s at around 500 psi and 20°C.

Table 5.4. Summary of the Experimental Results Compared to the Literature at 20°C

Average	Our Data MgH_2-$LaNi_5$-Nb_2O_5 (approx. 500 psi)	Au (2005) MgH_2-20 wt.% $LaNi_5$ (approx. 435 psi)	Srivastava (1999) $LaNi_5$ (approx. 730 psi)	Liu (2006) MgH_2 (approx. 1000 psi)
	HYDROGEN STORAGE CAPACITY (AT 20°C) (wt.%)			
Absorption	2.22	1.9	1.6	0.5
Desorption	2.02	1.7	1.5	0.2
	HYDROGEN STORAGE RATE (AT 20°C) (wt.%/s)			
Absorption	0.00152	0.000264	0.00148	0.0000694
Desorption	0.00127	0.0002236	0.000481	0.0000278

Compared to MgH_2-$LaNi_5$, MgH_2-$LaNi_5$-Nb_2O_5 composite material has higher absorption/desorption capacity and rate. In 2005, Au showed that MgH_2-$LaNi_5$ composite material has hydrogen storage capacity of 1.9 wt.% with a rate of 0.000264 wt.%/s and desorption capacity of the material was 1.7 wt.% with a rate of 0.000236 wt.%/s at 25°C and around 435 psi [3]. As mentioned before, both MgH_2-$LaNi_5$-Nb_2O_5 and MgH_2-$LaNi_5$ had 20 wt.% $LaNi_5$. Again, removing 7.3 wt.% of the MgH_2 and replacing it by Nb_2O_5 not only improved the absorption and desorption capacity, but also increased the rate of absorption/desorption rates of the composite material. The difference in absorption and desorption rates is even more clear, almost 5 times faster absorption and desorption were observed when 7.3 wt.% of the MgH_2 was replaced by Nb_2O_5.

Also, the absorption/desorption capacity and rate of the MgH_2-$LaNi_5$, MgH_2-$LaNi_5$-Nb_2O_5 composite material were compared to the $LaNi_5$ data from the literature. In 1999, Srivastava et al showed that using only $LaNi_5$ as hydrogen storage material gave a hydrogen storage capacity of 1.6 wt.% with a rate of 0.000148 wt.%/s and desorption capacity of the material was 1.5 wt.% with a rate of 0.000481 wt.%/s

at 33°C and around 730 psi [37]. The results showed that adding MgH_2 and Nb_2O_5 to $LaNi_5$ gave about 2 times higher hydrogen absorption/desorption capacity and 25 times higher absorption/desorption rate.

When the absorption/desorption capacity and rate of MgH_2-$LaNi_5$-Nb_2O_5 are compared to the data of MgH_2 in the literature, it can be seen that the new composite material has a higher absorption/desorption capacity and rate than MgH_2 alone [27]. In 2006, Liu et al showed that MgH_2 has hydrogen storage capacity of 0.5 wt.% with a rate of 0.0000694 wt.%/s and desorption capacity of the material was 0.2 wt.% with a rate of 0.0000278 wt.%/s at 25°C and around 1000 psi. Although the pressure used was two times higher than this work, adding $LaNi_5$ and Nb_2O_5 to MgH_2 significantly increased the hydrogen absorption/desorption capacity and rate. The new composite material worked a lot better than MgH_2 with 5 - 10 times higher absorption and desorption capacity and 40 times higher absorption/desorption rate at lower pressures.

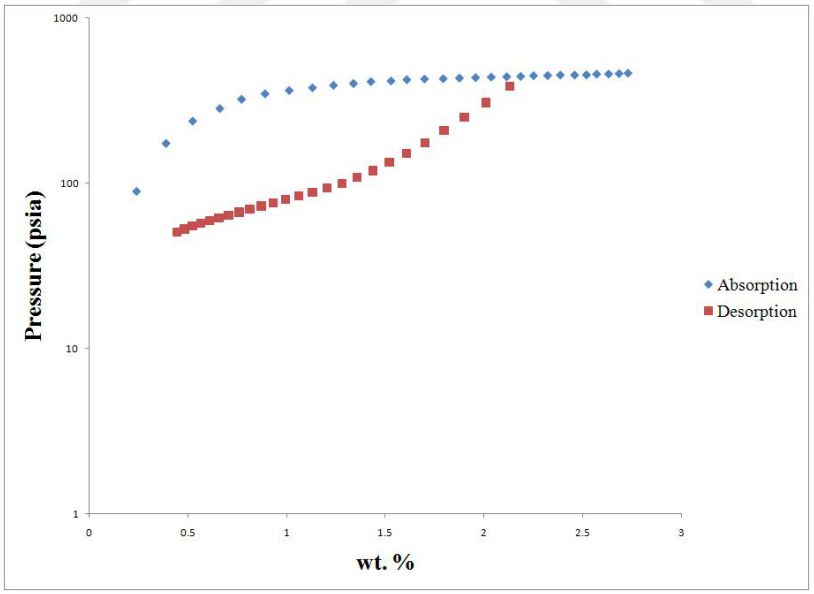

Figure 5.7. Absorption and Desorption PCI Curves at 20°C

In summary, the results of our experiments showed that our sorbent (MgH_2-20

wt.% $LaNi_5$-7.3 wt.% Nb_2O_5) has higher capacity for adsorption and shows higher rate of adsorption and desorption at different temperatures than the available sorbents in the literature today.

CHAPTER 6

CONCLUSIONS

This research study provided a better understanding of the effects of alloying $LaNi_5$ and Nb_2O_5 and with MgH_2. The rate and capacity of MgH_2-$LaNi_5$-Nb_2O_5 were measured by performing absorption and desorption experiments at different temperatures and the results were compared to the data in the literature.

- The results of our experiments showed that our sorbent (MgH_2-20 wt.% $LaNi_5$-7.3 wt.% Nb_2O_5) has higher capacity for adsorption and shows higher rate of adsorption and desorption at different temperatures than the available sorbents in the literature today.

- Our sorbent at a high temperature of 300°C showed that using both $LaNi_5$ and Nb_2O_5 together with MgH_2 increased absorption capacity and the rate. Using $LaNi_5$ in addition to MgH_2-Nb_2O_5 increases hydrogen storage capacity while using Nb_2O_5 together with MgH_2-$LaNi_5$ significantly increases the absorption and desorption rates. Adding $LaNi_5$ and Nb_2O_5 to MgH_2 increases the desorption rate and as well as hydrogen desorption capacity.

- Our sorbent at a moderate temperature of 100°C showed that our sorbent has a higher absorption/desorption rate and capacity. The positive effect of adding $LaNi_5$ and Nb_2O_5 to MgH_2 on absorption/desorpion capacity and rate was observed more prominently at lower temperatures.

- Our sorbent at a low temperature of 20°C showed the superior effect of alloying MgH_2 with $LaNi_5$ and Nb_2O_5 by dramatically increasing the hydrogen absorption/desorption rate and capacity, especially desorption rate and capacity.

CHAPTER 7

RECOMMENDATIONS

- To obtain optimum hydrogen absorption and desorption capacity and rate samples should be prepared and tested at different compositions of MgH_2, $LaNi_5$ and Nb_2O_5.
- To have a better understanding of the effect of ball-milling time and particle size on the rate and extend of hydrogen sorption and desorption, experiments using different ball-milling times, and particle size distributions, is recommended.
- To get better and more accurate experimental results, the experimental setup could be improved to provide constant temperature through the setup including the fresh hydrogen feed line and tank.
- To obtain a more accurate rate and extend of hydrogen sorption and desorption , the porosity of the sorbent could be taken into account to calculate the particle density.

BIBLIOGRAPHY

[1] "A Sustainable Energy Supply for Wales: Towards the Hydrogen Economy." *Hydrogen Wales* 2003: Web 26 Sept. 2009 ⟨http://www.h2wales.org.uk/⟩.

[2] Au, M., C. Chen, Z. Ye, T. Fang, J. Wu, and O. Wang. "The Recovery, Purification, Storage and Transport of Hydrogen Separated from Industrial Purge Gas by Means of Mobile Hydride Containers." *International Journal of Hydrogen Energy* 21.1 (1996): 33-37.

[3] Au, M., "Hydrogen Storage Properties of Magnesium Based Nanostructured Composite Materials." *Materials Science and Engineering B* 117.1 (2005): 37-44.

[4] Barkhordarian, G., T. Klassen, and R. Bormann. "Fast Hydrogen Sorption Kinetics of Nanocrystalline Mg Using Nb_2O_5 as Catalyst." *Scripta Materialia* 3rd ser. 49 (2003): 213-217.

[5] Berlouis, L. E. A., R. Perez Aguado, P. J. Hall, S. Morris, L. Chandrasekaran, and S. B. Dodd. "Dehydriding Kinetics of a Mg 9.5 wt. % V Sample Studied by High Pressure Differential Scanning Calorimetry." *Journal of Alloys and Compounds* 356-357 (2003): 584-587.

[6] Bhat, V. V., A. Rougier, L. Aymard, X. Darok, G. Nazri, and J. M. Tarascon. "Catalytic Activity of Oxides and Halides on Hydrogen Storage of MgH_2." *Journal of Power Sources* 159.1 (2006): 107-110.

[7] "BP's Statistical Review of World Energy Full Report 2009." *Scribd* 2009: Web 26 Sept. 2009 ⟨http://www.scribd.com/doc/16304689/BPs-Statistical-Review-of-World-Energy-Full-Report-2009⟩.

[8] Bunger, U., and W. Zittel. "Hydrogen Storage in Carbon Nanostructures Still a Long Road from Science to Commerce?" *Applied Physics A: Materials Science & Processing* 72.2 (2001): 147-151.

[9] "Carbon Capture Strategy Could Lead to Emission-Free Cars." *Georgia Institute of Technology* 2008: Web 27 Sept. 2009 ⟨http://www.gatech.edu/newsroom/release.html?id=1707⟩.

[10] Carter, T. J., and L. A. Cornish., "Hydrogen in Metals." *Engineering Failure Analysis* 8 (2001): 113-121.

[11] David, E., "An Overview of Advanced Materials for Hydrogen Storage." *Journal of Material Processing Technology* 162-163 (2005): 169-177.

[12] "DOE Seeks Applicants for Solicitation on the Employment Effects of a Transition to a Hydrogen Economy." *U.S. Department of Energy* 2006: Web 27 Sept. 2009 ⟨http://www1.eere.energy.gov/hydrogenandfuelcells/news_detail.html?news_id=9850⟩.

[13] Elam, C. C., C. E. Gregoire Padró, G. Sandrock, A. Luzzi, P. Lindblad, and E. Fjermestad Hagen. "Realizing the Hydrogen Future: the International Energy Agency's Efforts to Advance Hydrogen Energy Technologies." *International Journal of Hydrogen Energy* 28.6 (2003): 601-607.

[14] "Energy: Its Impact on the Environment and Society." *UK Dept for Business, Innovation and Skills (BIS)* 2006: Web 26 Sept. 2009 ⟨http://www.berr.gov.uk/energy/environment/energy-impact/page29982.html⟩.

[15] "Energy White Paper: Our Energy Future - Creating a Low Carbon Economy." *UK Dept for Business, Innovation and Skills (BIS)* 2003: Web 26 Sept. 2009 ⟨http://www.dti.gov.uk/energy/whitepaper/index.html⟩.

[16] Flynn, T. M., *Cryogenic Engineering.* 7th ed. Vol. 10. New York: Marcel Dekker, 1992.

[17] Garrett, D. E., *Chemical Engineering Economics.* New York: Van Nostrand Reinhold, 1989.

[18] Hart, D., *Hydrogen Power: The Commercial Future of the Ultimate Fuel.* London: Financial Times Energy, 1997.

[19] Hart, D., P. Freund, and A. Smith. "Hydrogen - Today and Tomorrow." *IEA Greenhouse Gas R&D Programme* 2003: Web 15 Sept. 2009 ⟨http://www.ieagreen.org.uk/hydrogen.pdf⟩.

[20] Heffel, J. W., "NO_x Emission and Performance Data for a Hydrogen Fueled Internal Combustion Engine at 1500 rpm Using Exhaust Gas Recirculation." *International Journal of Hydrogen Energy* 28.8 (2003): 901-908.

[21] Huot, J., G. Liang, S. Boily, A. Van Neste, and R. Schulz. "Structural Study and Hydrogen Sorption Kinetics of Ball-Milled Magnesium Hydride." *Journal of Alloys and Compounds* 293-295 (1999): 495-500.

[22] "Hydrogen Basics - Production." *Florida Solar Energy Center* Web 26 Sept. 2009 ⟨http://www.fsec.ucf.edu/en/consumer/hydrogen/basics/production.htm⟩.

[23] "Hydrogen, Fuel Cells and Infrastructure Technology Program - Multiyear Research, Development and Demonstration Plan." *U.S. Department of Energy* 2003: Web 26 Sept. 2009 ⟨http://www1.eere.energy.gov/hydrogenandfuelcells/fuelcells/⟩.

[24] "Hydrogen Production and Storage: R&D Priorities and Gaps" *International Energy Agency Hydrogen Coordination Group* 2006: Web 15 Sept. 2009 ⟨http://www.iea.org/Textbase/papers/2006/hydrogen.pdf⟩.

[25] Kim, J. W., J. P. Ahn, S. A. Jin, S. H. Lee, H. S. Chung, J. H. Shim, Y. W. Cho, and K. H. Oh. "Microstructural Evolution of NbF_5-Doped MgH_2 Exhibiting Fast Hydrogen Sorption Kinetics." *Journal of Power Sources* 178.1 (2008): 373-378.

[26] Latroche, M. "Structural and Thermodynamic Properties of Metallic Hydrides Used for Energy Storage." *Journal of Physics and Chemistry of Solids* 65.2-3 (2004): 517-522.

[27] Liu, Y., Z. Xiong, J. Hu, G. Wu, P. Chen, K. Murata, and K. Sakata. "Hydrogen Absorption/Desorption Behaviors Over a Quaternary Mg-Ca-Li-N-H System." *Journal of Power Sources* 159.1 (2006): 135-138.

[28] McCarthy, J.,"Hydrogen." *Formal Reasoning Group* 2008: Web 27 Sept. 2009 ⟨http://www-formal.stanford.edu/jmc/progress/hydrogen.html⟩.

[29] "Metal Hydride." *Hydrogen Components, Inc.* Web. 27 Sept. 2009. ⟨http://www.hydrogencomponents.com/hydride.html⟩.

[30] Noganow, L. S., "Hydrogen." *McGraw-Hill Encyclopedia of Science & Technology.* 7th ed. Vol. 8. New York: McGraw-Hill, 1992. 581-588.

[31] Price, T. E C., D. M. Grant, I. Telepeni, X. B. Yu, and G. S. Walker. "The Decomposition Pathways for $LiBD_4$ - MgD_2 Multicomponent Systems Investigated by *in situ* Neutron Diffraction." *Journal of Alloys and Compounds* 472.1-2 (2009): 559-564.

[32] "Prospects for a Hydrogen Economy." *Parliamentary Office of Science and Technolog* 2002: Web 26 Sept. 2009 ⟨http://www.parliament.uk/parliamentary_offices/post/pubs2002.cfm⟩.

[33] Rodewald, U. C., B. Chevalier, and R. Pöttgen. "Rare Earth - Transition Metal - Magnesium Compounds - An Overview." *Journal of Solid State Chemistry* 180.5 (2007): 1720-1736.

[34] "Route Map Paper Hydrogen." *UK Dept for Business, Innovation and Skills (BIS)* 2002: Web 26 Sept. 2009 ⟨http://www.dti.gov.uk/renewable/routemap.htm⟩.

[35] Solomon, B. D., and A. Banerjee. "A Global Survey of Hydrogen Energy Research, Development and Policy." *Energy Policy* 34.7 (2006): 781-792.

[36] Sorensen, B., "Handling Fluctuating Renewable Energy Production by Hydrogen Scenarios." *Danish Hydrogen Committee, Roskilde University* 2002

[37] Srivastava, S., and O. N. Srivastava. "Hydrogenation Behaviour with Regard to Storage Capacity, Kinetics, Stability and Thermodynamic Behaviour of Hydrogen Storage Composite Alloys, $LaNi_5/La_2Ni_7$, $LaNi_3$." *Journal of Alloys and Compounds* 290.1-2 (1999): 250-256.

[38] Tanaka, K. "Hydride Stability and Hydrogen Desorption Characteristics in Melt-Spun and Nanocrystallized Mg-Ni-La Alloy." *Journal of Alloys and Compounds* 450.1-2 (2008): 432-439.

[39] "Technology White Paper on Generation of Hydrogen and Transportation and Transmission of Energy Generated on the U.S. Outer Continental Shelf to Onshore." *OCS Alternative Energy and Alternate Use Programmatic EIS Information Center* U.S. Department of the Interior, 2006: Web 26 Sept. 2009 ⟨http://ocsenergy.anl.gov⟩.

[40] Thomas, D., "Strategic Study of Renewable Energy Resources in Wales." *Sustainable Energy Ltd* (2001): Draft Report

[41] Worf, J. C. "Metal Hydrides." *McGraw-Hill Encyclopedia of Science & Technology.* Vol. 11. New York: McGraw-Hill, 1992. 37-41.

[42] Wu, C. Z., P. Wang, X. Yao, C. Liu, D. M. Chen, G. Q. Lu, and H. M. Cheng. "Effect of Carbon/Noncarbon Addition on Hydrogen Storage Behaviors of Magnesium Hydride." *Journal of Alloys and Compounds* 414.1-2 (2006): 259-264.

[43] Yvon, K. and P. Fischer, "Crystal and Magnetic Structures of Ternary Metal Hydrides: A Comprehensive Review." *Hydrogen in Intermetallic Compounds - Electronic, Thermodynamic, and Crystallographic Properties, Preparation (Topics in Applied Physics).* Vol. 63. New York: Springer, 1988. 87-138.

[44] Zaluska, A., L. Zaluski, and J. O. Ström - Olsen. "Nanocrystalline Magnesium for Hydrogen Storage." *Journal of Alloys and Compounds* 288.1-2 (1999): 217-223.

[45] Zhenglong, L., L. Zuyan, and C. Yanbin. "Cyclic Hydrogen Storage Properties of Mg Milled with Nickel Nano - Powders and NiO." *Journal of Alloys and Compounds* 470.1-2 (2009): 470-472.